

OPTIMIZATION AND RE-DESIGN OF A WHEEL HUB TO REDUCE UNSPRUNG MASS OF A RALLYCROSS CAR

Bachelor Degree Project in Mechanical Engineering
C-Level 30 ECTS
Spring term 2018

Emil Andersson

Supervisor: Ulf Stigh
Examiner: Lennart Ljungberg
Client: EKS

Abstract

The Wheel Hub of a rallycross car is analysed to reduce the unsprung mass of the car. The problem statement is to mainly focus on the unsprung mass related to the suspension, and more specifically on the Wheel Hub. One of the objectives of the suspension system of a car is to damping the movement of the car. This is an important area when designing a vehicle, and especially a race car due to the extreme conditions that may result in reduced traction and loose of confidence for the driver. A theoretical model is performed to demonstrate the importance of a low unsprung mass and to illustrate how it affects the vehicle-handling. A process to evaluate the current Wheel Hub and decision to re-design the Wheel Hub is performed, and the parts are analysed using the Finite Element Method to verify the design and material selection. Vehicle dynamics of the car is analysed to calculate the acting forces. Optimization of the design is performed by using Computer Aided Engineering. The re-designed Wheel Hub presented as the result of this project with a Brake Disk Adapter integrated in Hub. This design reduces the number of parts, and the unsprung mass up to 25% without any effects on suspension geometry or other parts of the car.

Keywords: *Wheel Hub, vehicle dynamics, optimization, Finite Element Analysis*

Certification

This thesis has been submitted by Emil Andersson to the University of Skövde as a requirement for the degree of Bachelor of Science in Mechanical Engineering. The undersigned certifies that all the material in this thesis that is not my own has been properly acknowledged using accepted referencing practices and, further, that the thesis includes no material for which I have previously received academic credit.

Any Design protection of the outcome in this thesis is handed over to the client to investigate before manufacturing, and the author will not be responsible for any suspicions about plagiarism regarding the design.

Emil Andersson

Skövde 2018-06-19

Department of Engineering Science

Acknowledgements

First, a big thanks to Janne Ljungberg at EKS that give me the opportunity and trust to make this project. Thanks also to all my study friends that helps me through the study with discussions, tips and corrections.

My supervisor Ulf Stigh at University of Skövde with his wide knowledge in the theoretical aspects and the support of how to face my problems and questions.

My family and friends for being so persevering in this project, and my years at the university.

Thank you!

Emil Andersson
Skövde, 2018-06-19

Table of Contents

Abstract	i
Certification	ii
Acknowledgements	iii
List of Figures	vi
List of Figures Appendices	vii
List of Tables	vii
List of Tables Appendices	vii
Nomenclature	viii
Software's used	viii
1 Introduction	1
1.1 Technology, Society and Environment	1
1.2 About EKS RX/EKS	2
1.3 Rallycross - The discipline	2
2 Background	3
2.1 Problem Statement	3
2.1.1 Aims for the project	3
2.1.2 Limitations	4
3 Overview of the thesis	4
3.1 The Wheel Hub - Function	4
3.1.1 Current design	5
3.1.2 Current design masses	7
3.1.3 Wheel Hub from Pankl Systems AG	7
4 Method and Approach	7
4.1 Comparative Design Analysis	8
4.2 Concept Screening	9
4.3 System Optimization	10
4.4 Structural Optimization	10
4.5 Terminology and Standard SAE J670	10
4.6 Definition of Sprung and Unsprung masses	11
4.7 Theoretical and mathematical models	11
4.7.1 Mass spring system of Quarter-Car Model	12
4.7.2 MATLAB® and Simulink® simulation	12
4.8 Materials	13
4.8.1 Current Material used in Wheel Hub, Socket and Tap	14
4.9 Calculation of acting loads	15
4.9.1 Assumptions made in the calculations and Finite Element Analysis	15
4.9.2 Dimensions	15
4.9.3 Data Analysis	16
4.9.4 Forces - Normal conditions	19
4.9.5 Acceleration torque	20
4.9.6 Braking torque	21
4.9.7 Forces - Impact forces and Special cases	22

4.9.8	Heat load.....	23
4.10	Safety Factor.....	24
4.11	Finite Element Analysis and Optimization.....	25
4.11.1	Loads used in the Finite Element Analysis	26
4.11.2	Finite Element Analysis of Wheel Hub - Current design.....	26
4.11.3	Finite Element Analysis of Brake Disk Adapter - Current design	27
4.11.4	Finite Element Analysis of Socket - Current design	28
4.12	Design Analysis of the current Hub and Brake Disk Adapter.....	28
4.12.1	Finite Element Analysis, Re-design and Optimization of the new Hub.....	30
5	Results and Discussion of the Re-designed Wheel Hub	39
5.1	New designed Wheel Hub - With Brake Disk Adapter integrated.....	41
5.2	Threads discussed for the CV-joint and Cup.....	41
5.3	Centring ring for the rim	42
5.4	Interfaces for Brake Disk	42
5.5	Cup	43
5.6	Tap.....	44
5.7	Masses of the current design, the Optimized and Re-designed Wheel Hub's.....	44
5.8	Simulation of the results in MATLAB® and Simulink®	45
6	Discussion.....	46
6.1	Type of data collected from the car.....	46
6.2	Accuracy of the loads.....	46
6.3	Material properties - uncertainty	47
6.4	Selection of material.....	47
6.5	Long Time/fatigue - neglected	47
6.6	CAD-models.....	47
6.7	Re-designed Hub and Cup.....	47
7	Conclusions and Recommendations	48
8	Future Work	48
	References	49
	Appendices	A-1
	Work Breakdown and Time Plan - Before project start	A-1
	Work Breakdown and Time Plan - After project comments	A-3
	Project Risk Analysis	A-4
	Project Risk Analysis - After project comments	A-5
	Drawing Current Hub.....	A-6
	Drawing Current Socket.....	A-7
	Drawing Brake Disk from Brembo®	A-8

List of Figures

Figure 1.1. Rallycross-track Mettet, Belgium 2018.....	2
Figure 3.1. Complete Wheel Hub, upright and driveshaft.....	4
Figure 3.2. Current Wheel Hub.....	5
Figure 3.3. Current Wheel Hub and Brake Disk Adapter.....	6
Figure 3.4. Current Tap.....	6
Figure 3.5. Ring, Screws and Brake Disk Adapter.....	6
Figure 3.6. Assembled section-view of the Wheel Hub.....	7
Figure 3.7. Pankl System Wheel Hub.....	7
Figure 4.1. Flowchart of methodology.....	8
Figure 4.2. Concept Hub - 1.....	9
Figure 4.3. Concept Hub - 2.....	10
Figure 4.4. Concept Hub - 3.....	10
Figure 4.5. Coordinate System and roll, pitch, yaw - Definition.....	11
Figure 4.6. 2D-mass spring system.....	12
Figure 4.7. Simulation plot from Simulink of two different unsprung masses - Position.....	13
Figure 4.8. Damper positions.....	17
Figure 4.9. Damper position - mean front and rear.....	17
Figure 4.10. Roll and pitch from data analysis.....	18
Figure 4.11. Centre of Gravity change in position.....	18
Figure 4.12. Free Body Diagram y-z-plane.....	19
Figure 4.13. Free Body Diagram x-z-plane.....	19
Figure 4.14. Forces normal conditions.....	20
Figure 4.15. Forces on Hub and wheel.....	20
Figure 4.16. Free Body Diagram Torque applied.....	21
Figure 4.17. Speed vs. Time.....	21
Figure 4.18. Free Body Diagram Braking.....	22
Figure 4.19. Forces acting on the car at one wheel.....	23
Figure 4.20. Tetrahedral element.....	25
Figure 4.21. Tetrahedral elements mesh - Hub.....	25
Figure 4.22. Tetrahedral elements mesh - Cup.....	26
Figure 4.23. von Mises stresses in current Hub [MPa].....	27
Figure 4.24. von Mises stresses in current Hub with heat load [MPa].....	27
Figure 4.25. von Mises stresses in Current Brake Disk Adapter [MPa].....	28
Figure 4.26. von Mises stresses in current Socket [MPa].....	28
Figure 4.27. Wheel Hub backside of rim attachment area.....	29
Figure 4.28. Hub centring ring.....	29
Figure 4.29. Current Brake Disk Adapter on the car 2018.....	30
Figure 4.30. Brake Disk Adapter 2017.....	30
Figure 4.31. Re-designed Wheel Hub - Assembly.....	31
Figure 4.32. Boundary Conditions - Hub.....	32
Figure 4.33. Areas that have been optimized in the Hub.....	32
Figure 4.34. von Mises stresses - Cup in Steel C55 or 15CDV6 [MPa].....	33
Figure 4.35. von Mises stresses - Cup in Aluminium 7075-T6 [MPa].....	33
Figure 4.36. von Mises stresses [MPa].....	34
Figure 4.37. von Mises stresses detailed view [MPa].....	34
Figure 4.38. von Mises stresses deformed 20% scaled [MPa].....	35
Figure 4.39. Max Principal Strain in the Hub.....	35

Figure 4.40. Displacement Magnitude [mm]	36
Figure 4.41. Displacement Magnitude deformed 20% scaled [mm]	36
Figure 4.42. Failure Index - Hub	37
Figure 4.43. Assembled Wheel Hub Boundary Conditions	37
Figure 4.44. Assembled Wheel Hub von Mises stresses deformed 20% scaled [MPa]	38
Figure 4.45. Assembled Wheel Hub von Mises stresses deformed 20% scaled [MPa]	38
Figure 4.46. Assembled Wheel Hub von Mises stresses deformed 20% scaled detailed view [MPa] ..	38
Figure 5.1. Result of Current and Re-designed Hub's	39
Figure 5.2. Re-designed Wheel Hub - Assembly	40
Figure 5.3. Skeleton section of the Hub	41
Figure 5.4. Right-Hand and Left-Hand threads defined	41
Figure 5.5. Wheel Hub - New design	42
Figure 5.6. Wheel Hub and Brake Disk - Exploded view (Half-view)	43
Figure 5.7. Wheel Hub and Brake Disk - Assembled (Half-view)	43
Figure 5.8. Cup	43
Figure 5.9. Cup assembled in the Wheel Hub (Quarter section-view of Hub)	44
Figure 5.10. Re-designed Tap	44
Figure 5.11. CV-joint with re-designed Tap	44
Figure 5.12. Current and Aluminium Sockets	45
Figure 5.13. Simulation plot from Simulink of the different unsprung masses in Table 5.1 - Position.	46

List of Figures Appendices

Figure A-1. Gantt Plan Full Project	A-1
Figure A-2. Gantt Plan Pre-study	A-2
Figure A-3. Gantt Plan Development process	A-2
Figure A-4. Gantt Plan Development process - After project	A-3
Figure A-5. Drawing Current Hub	A-6
Figure A-6. Drawing Current Socket	A-7
Figure A-7. Drawing Brake Disk from Brembo®	A-8

List of Tables

Table 4.1. Comparative Design Analysis	9
Table 4.2. Material Data	13
Table 4.3. Chemical Properties of materials	14
Table 4.4. Parameters for calculations of acting loads	16
Table 4.5. Rating Number and sum of RN	25
Table 4.6. Dimensioning forces and torques	26
Table 4.7. Margin of Safety	39
Table 5.1. Specific masses - Current, Optimized and Re-designed Wheel Hub's	45

List of Tables Appendices

Table A-1. Project Risk Analysis	A-4
--	-----

Nomenclature

F = Force [N]

F_{fric} = Friction force [N]

M = Total mass [kg]

m_{us} = Unsprung mass [kg]

m_s = Sprung mass [kg]

a = Acceleration [m/s²]

W = Road input/displacement [mm]

CGH = Centre of Gravity height [mm]

t = Time [sec]

v = Velocity [m/s]

g = Gravity 9.81 [m/s²]

μ = Friction coefficient

θ = Roll angle [°]

Φ = Pitch angle [°]

γ = Yaw angle [°]

N = Normal force [N]

I = Moment of Inertia [kgmm²]

$F_{calculated}$ = Force calculated from data analysis [N]

F_n^{SF} = Force with applied Safety Factor [N]

T = Torque/moment [Nm]

Δ = Difference

F_{fric} = Friction force [N]

α = Angular acceleration [rad/s²]

s = Sum of Rating Number (RN)

SF = Safety Factor

Wr = Wheel radius [mm]

z = Position [mm]

x = Distance [m]

Wb = Wheel base [mm]

Tw = Width of track [mm]

H = Height [mm]

Ww = Wheel width [mm]

$\bar{\bar{R}}$ = Rotation matrix

$\frac{d}{dt}$ = Derivative with respect to time

Software's used

PTC Creo Parametric 4.0 - Modelling CAD and perform Finite Element Analysis

MathWorks MATLAB® and Simulink® 2015 - Numerical computation for calculations and model simulations

Granta Design CES EduPack 2017 - Material selection and evaluation of environmental impact

Microsoft Office Word 2016 - Text processing, grammar control and finalisation of thesis

Microsoft Office Excel 2016 - Compilation of tables

1 Introduction

In rallycross only one thing counts - to be fastest. Everything need to be in harmony. A driver has to be such comfortable with the behaviour of the car that he, or she can set the limits of its performance. Engineers all over the world still fascinated of the topic Sir Isaac Newton (1642-1727) presents in "Principia Mathematica Philosophiae Naturalis" in 1686, and his three laws of motions. Newton shown that the "*The force is equal to the change in momentum per change in time. For a constant mass, force equal mass times acceleration*". The force F acting on a body is related to its mass M and the acceleration a . see Equation (1.1) (Jansson & Grahn, 2013), (NASA, 2018).

$$F = Ma = M \frac{dv}{dt} \quad (1.1)$$

The importance is to complete a specified distance in shortest possible time, the velocity is important. The velocity is the change in distance x with respect to time t required, see Equation (1.2) (Jansson & Grahn, 2013), (NASA, 2018). The relation of this equations is that the mass and the force is important to complete the distance in a short time.

$$v = \frac{\Delta x}{t} \quad (1.2)$$

The force F in Equation (1.1) given from the combustion engine has a specified value, and the mass of the car. Therefore, every detail of the car is important in terms of mass and performance.

When traveling along the circuit, within a corner and acceleration the friction F_{fric} between tire and surface is important. The friction coefficient μ and Gravity g is constant, so the normal force N is governing parameter in the friction equation, see Equation (1.3) (Jansson & Grahn, 2013).

$$F_{fric} = \mu N = \mu M g \quad (1.3)$$

If the normal force for some reason is disturbed by a change in the contour of the surface, the normal force goes to zero, and thus also the friction force - loses contact and traction. This is an undesirable phenomenon and related to Equation (1.1). If the mass is decreased within equal force, the particle gains a higher acceleration, and can follow the contour of the surface smoother to keep the friction force intact.

1.1 Technology, Society and Environment

Sustainable development is commonly described as "*development that meets present needs without compromising the ability of future generations to meet their own needs*" (The International Institute for Sustainable Development (IISD), 2018). Everything engineered and manufactured need to be carefully considered due to the TSE - Technology, Society and Environment effects. The objectives of this project are to reduce the total mass of the car. In the rallycross car, this is made to perform a better acceleration, braking and cornering. In road or passenger cars a low mass will reduce the amount of energy, or fuel used to transport the car a desired distance. The knowledge in motorsport and thought this project will be applied in performance cars, but also normal passenger cars. Car manufacturer trying to reduce the fuel consumption to increase the number of sold cars because of reduced exhaust emissions. By using new technology, the amount of material with retained strength can reduce the need of both experimental testing of physical models and the raw material to produce the product. With increased computational capabilities the possibilities to perform simulations that realizes the physical model, which reduces the time in both engineering development and manufacturing processes.

1.2 About EKS RX/EKS

From the web site of EKS:

“To most people, Mattias is best known as a champion of the Deutsche Tourenwagen Masters (DTM). He won the championship for Audi in 2004 and 2007 and he was overall first runner-up in 2014 and 2017. Apart from driving in DTM, Mattias has won race titles all over the world. The idea of creating a privately-owned rallycross team was put to paper in late 2013. The plan was to compete in the FIA World Rallycross Championship in 2014. People in the business said it would take one and a half to two years to build a rallycross car. And even then, it wouldn't be enough time to have a ready-to-race car with top-level performance. To say it was a challenge would be an understatement. The team signed up as EKS, three-letter code of Mattias Ekström in DTM. After having the engine flown in by helicopter from Sweden, the mechanics completed the last finishing details just in time for the start – the first Audi S1 EKS RX car was ready to race. A month later, Mattias ended up at the top of the podium in Höljes, Sweden. It had only been six months since the team started working in an empty garage in Fagersta, Sweden. The perception that it was an “impossible project” just added fuel to the desire to show the know-it-all the opposite. In late 2016, three years into the project, Mattias could call himself World Champion and - as if that hadn't been enough already - EKS won the Team's Championship” (EKS RX, 2018).

1.3 Rallycross - The discipline

To introduce the rallycross-discipline a short description is given:

Rallycross is a combination of rallying and circuit racing. It is head-to-head racing on mixed surfaces of gravel (40%) and tarmac (60%) (EKS RX, 2018). Short and intensive racing in about four to six minutes with several competitors starting at the same time gives a close racing and often contact between the cars. A rallycross-supercar that EKS uses is a four-wheel drive car with a two litres turbo-charged engine (EKS RX, 2018). A typical rallycross-track Circuit Jules Tacheny, Belgium is shown in Figure 1.1 (EKS RX, 2018).



Figure 1.1. Rallycross-track Mettet, Belgium 2018 (EKS RX, 2018)

2 Background

2.1 Problem Statement

The problem statement for this project is mainly to focus on the unsprung mass of the car, and more specific the Wheel Hub. The suspension of a car is designed with objects to isolate and damping vibrations produced from the road disturbance (Sharma, Saluja, Saini, & Saini, 2013). The vibrations of the car are an important area to concern when design a vehicle, and especially a race car due to the extreme conditions the car is moving in. Relations between the comfort of a passenger car and the performance can be made, a bumpy ride for a passenger can in many cases result in less traction and loose of confidence for a driver. For road cars, speed humps and pot holes are the main cause of vibrations of the car through the tire/wheel and the suspension (Sharma & Nain, 2015). In race cars, even harder environments can appear with big jumps and impacts from other competitors. By making mathematical models of the car, the behaviour of the masses can be analysed when the car travel over a bump (Galal, 2015). A Dynamic Quarter-Car Model in two degrees of freedom can be used as a simplification for a full car model-analysis and response when the car caused by a road distribution (Sharma, Saluja, Saini, & Saini, 2013).

EKS have an idea of how to make another design for the Wheel Hub used on the car today to gain a lower unsprung mass with retained strength. The Wheel Hub is an important part of the car and the suspension. EKS have the aims to improve the car at every part and the suspension is a key-point to develop.

2.1.1 Aims for the project

- **Estimation of acting loads**
Based on previous real data from the car, calculate the forces applied on the Wheel Hub. Forces and moments from chassis, drivetrain and suspension need to be analysed to make an accurate simulation.
- **Comparative Design Analysis**
Compare two types of Wheel Hub designs, regarding the advantages, and disadvantages of the designs.
- **Optimization**
The current Wheel Hub can be optimized with knowledge from the other designs. This should be performed with CAD-models, CAD means Computer Aided Design. EKS will provide CAD-models including drawings of all interesting parts. Finite Element Analysis will be performed, mathematical analysis and optimization to find an optimal design with reduced mass, required strength, and usability during service of the car. EKS can contribute with examples of other solutions, contact with peoples that have knowledge and data from previous experiences and tests.
- **New design**
Perform a design concept of a new Wheel Hub or present what changes can be done with the current Hub to obtain the desired improvement. The design need to be optimized with respect to total mass and fulfils the requirements of function.

Targets in the project is mass loss gain vs. performance, and the advantages of making a new Wheel Hub. The design shall be evaluated due to the performance, mass (economic is not considered in this project) and what types of changes are worth implementing.

2.1.2 Limitations

Due to the limited time of the thesis work some parts need to be neglected in the process. The thesis work project is restricted and limited to not make any geometrical changes that effects the suspension geometry or other components in the car. Parts as the CV-joint where CV stands for Constant Velocity, and the Wheel Bearing will be analysed in terms of usefulness, due to the design aspects of the re-designed Wheel Hub before any deeper analysis of each part will be performed.

The time for the project is limited to 20 weeks and includes 30 ETCS-credits.

3 Overview of the thesis

A rallycross car Wheel Hub is analysed to reduce the mass. In this project “Wheel Hub” is the assembled part and “Hub” is the specific part. A mathematical model is performed to show the importance of low unsprung mass of a car. A development process described to fulfil the objectives to reduce the mass of the Wheel Hub and containing parts. The process starts with a Comparative Analysis, Concept Screening and Structural/Topology Optimization is performed to methodically work out a design that meets the requirements. High-strength Steels as Alloy 15CDV6 and 300M are discussed in the selection of finding a material that satisfies the requirements of the Wheel Hub. Alternative materials as plastic is discussed, and Aluminium 7075-T6 is deeply analysed in parts which are not affected by large forces. The forces and loads acting on the Wheel Hub and containing parts are analysed through a vehicle dynamic analysis in both two- and three dimensions. The uncertainties due to the assumptions and simplifications made in the calculations is covered by a Safety Factor. The selection of Safety Factor is made with respect to the uncurtains in calculations, material properties, manufacturing and effects of failures. A Finite Element Analysis with optimization tools in CAD-software is performed to evaluate the design.

3.1 The Wheel Hub - Function

The Wheel Hub, in most applications the centre of a wheel, or other rotation components. The Hub mainly used to attach a bearing which allows the wheel to rotate around an axle. The bolt and attachment for the wheel is a part of the Wheel Hub. Wheel Hub's located at a driven axle of the car transfer torque from the driveline to the wheel. The Wheel Hub's on the rallycross car is equal due to cost reduction and the fact that the car is four-wheel-driven. The current assembled Wheel Hub with upright, which is a part of the suspension that attaches the Hub, the strut and the control arms and driveshaft included is presented in Figure 3.1.

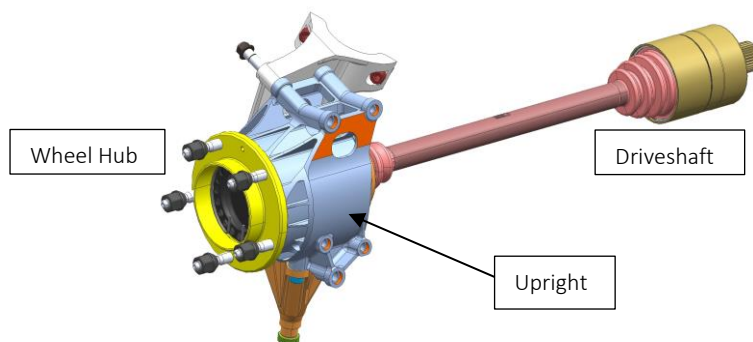


Figure 3.1. Complete Wheel Hub, upright and driveshaft

3.1.1 Current design

The current product contains eight parts. Parts included in the Wheel Hub, see Figure 3.2. The Tap presented in Figure 3.4 which also contains the Brake Disk Adapter, number 6.

A Ring fixed with M5 Screws locks the Brake Disk in axial direction, see Figure 3.5 which also includes the backside of the Brake Disk Adapter.

Nomenclature and function of parts included:

- 1) **Hub**
Used to transfer the moment from the driveshaft via the CV-joint to the wheel/rim. Attachment for the rim
- 2) **CV-joint**
To transfer moment from driveshaft (from engine/gearbox) to Hub without a predictable angle of steering. (This part is not included in the analysis or discussions)
- 3) **Socket**
Holding the CV-joint in place inside the Hub.
- 4) **Retaining ring**
Locks the Socket in place.
- 5) **Tap**
Seal the CV-joint from dust and damp. Fixture to retaining spring for the driveshaft.
- 6) **Brake Disk Adapter**
Is used to assemble the Brake Disk, see Figure 3.3 for assembled Brake Disk.
- 7) **Ring**
Ring to fix the Brake Disk in axial direction.
- 8) **Screw**
To hold the Ring in place.



Figure 3.2. Current Wheel Hub

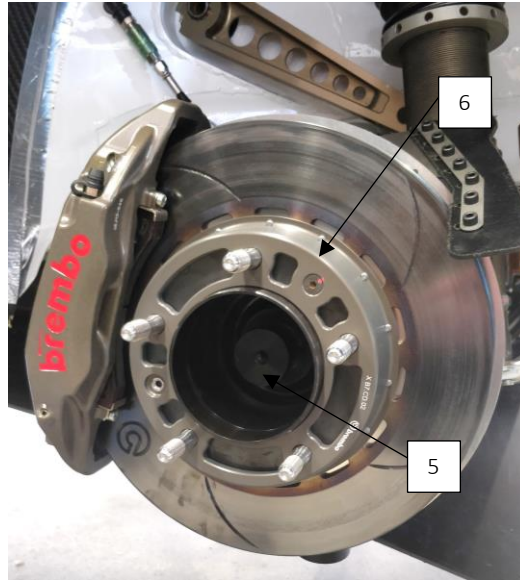


Figure 3.3. Current Wheel Hub and Brake Disk Adapter



Figure 3.4. Current Tap

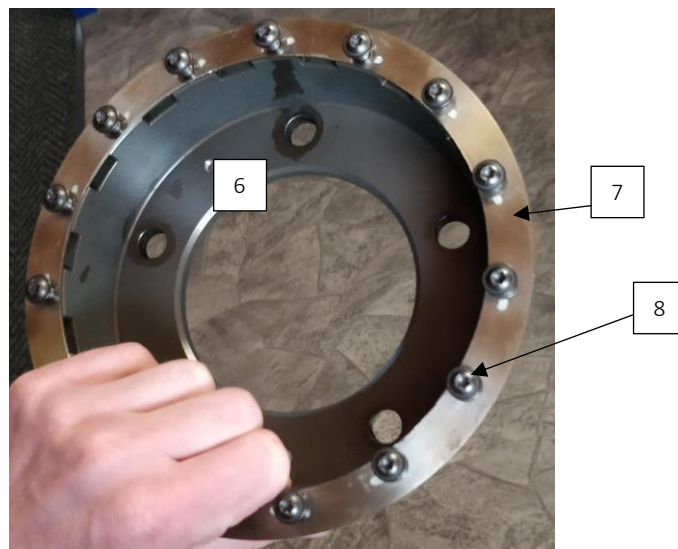


Figure 3.5. Ring, Screws and Brake Disk Adapter

To show all parts discussed, the Figure 3.6 presents a section-view with all parts against the Brake Disk Adapter tightly assembled as used on the car. Each part has the number (1-8) shown in the list of containing parts.

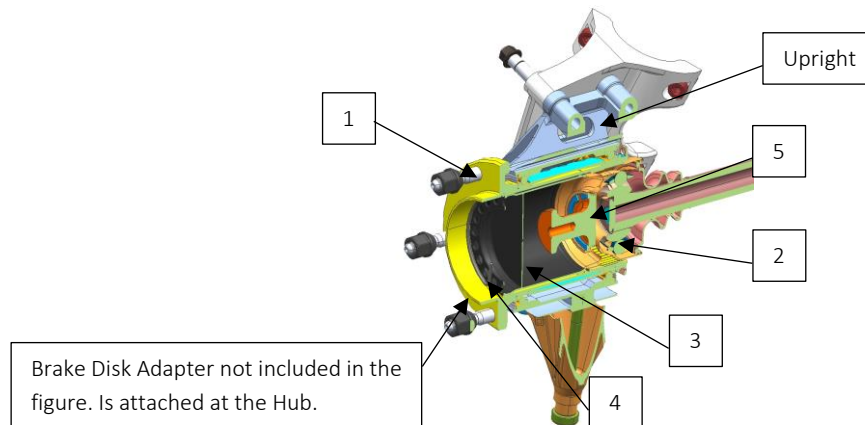


Figure 3.6. Assembled section-view of the Wheel Hub

3.1.2 Current design masses

The main objectives in this project is to reduce the mass, both the total mass and the unsprung mass of the Wheel Hub, with retained strength and function. Therefore, all containing parts are analysed in the Pre-study to define the current masses. The current parts are both measured in experiments by a scale and measured in Creo, this due to investigate the accuracy of the measurements made in Creo. The new designs are only measured in Creo. The masses presented in Section 5 due to its relevance in comparing the current and re-designed Wheel Hub's, see Table 5.1.

3.1.3 Wheel Hub from Pankl Systems AG

EKS has interest in other types of Wheel Hub designs used in other rally/racing cars. The Wheel Hub developed and manufactured by the Austrian company Pankl System AG and used on the Ford Fiesta WRC/S2000-rally cars. Pankl Systems are informed that EKS are interested in the design, but no further information regarding patent or design protection are discussed in this state. The design is not aimed to be copied, and only used as inspiration of a new Wheel Hub to EKS.

This Wheel Hub is manufactured in a one-piece model to make the number of parts and the mass can be reduced significantly. See Figure 3.7 for pictures of the design in three angles; top, side and bottom.

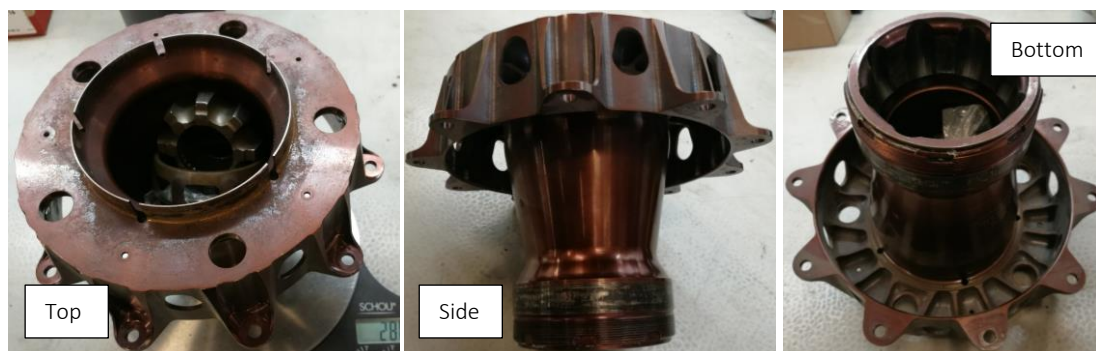


Figure 3.7. Pankl System Wheel Hub

4 Method and Approach

To fulfil the objectives of this project in a time effective way, the main work divided in the steps; Concept Screening, System Optimization and Structural Optimization. See Figure 4.1 for the flowchart of the methodology that will be used (Wollstrand & Sallbring, 2015).

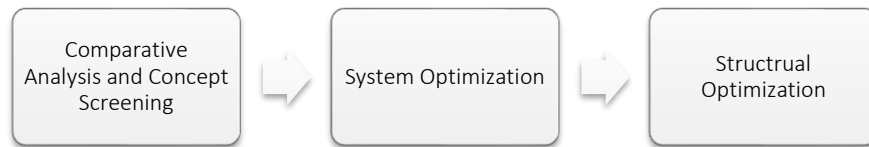


Figure 4.1. Flowchart of methodology

- **Comparative Analysis and Concept Screening**

The Wheel Hub are analysed by testing design variation with background from other Wheel Hub designs and knowledge from the author and EKS. The designs are performed with simple CAD models for visualization. Every interesting detail and ideas collected in this phase.

- **System Optimization**

Each design concept from the Screening are validated and investigated for the most optimal design variations. The goal to fulfil the objectives to minimize the mass and number of part if possible. An algorithm to select the designs to proceed with are used.

- **Structural Optimization**

The design concepts are developed as precise CAD-models. Finite Element Analysis are performed of the models to investigate the design in strength and mass aspects. A Structural Optimization is performed to consider an optimal design. The design concepts are condensed to one or two concept that fulfils the objectives in the project.

4.1 Comparative Design Analysis

The two Wheel Hub designs that EKS consider interesting are compared to find the advantages and disadvantages. The current design from the Audi S1 EKS RX are compared to a Wheel Hub from a Ford Fiesta S2000/WRC manufactured by Pankl Systems Racing AG and provided by EKS. The “S2000” and “WRC”-cars are two International rally regulations and therefore the same type of cars. This analysis is interesting to perform both on the current Wheel Hub and another Hub, in this project from Pankl Systems to evaluate the design aspects. The current Wheel Hub may have advantages in some features that need to be considered in the development process to find an optimal design.

The analysis is performed with;

- **Mechanical use-perspective**

By comparing the designs in mechanical use-perspective the Wheel Hub’s are evaluated due to usefulness for the mechanics to work. The Hub is required to work with several other parts on the car, and they may need to be changes with less work-effort as possible.

- **Engineering perspective**



The number of parts, and the design regarding amount of material/mass used. These features are interesting to compare, and to understand which changes in the design that can reduce the number of parts and mass.

The price is not considered in this project and analysis. Table 4.1 shows the Comparative Analysis, and the advantages and disadvantages of the Hub’s which are compared. From discussions with EKS (Ljungberg, 2018) the advantages, and disadvantages of the Hub’s are performed. The aspects of features in the two designs is used in the development of a new Hub to set focus on important parts of the design, and therefore it is important to evaluate both in the Pre-study.

The total mass of the current Wheel Hub, and Pankl Racing-Hub is given with the CV-joint included compared to the mass in Table 5.1 later discussed. The both designs have their advantages and disadvantages, but the low mass of the Ford Fiesta-Wheel Hub from Pankl Systems, and the number of

parts is the interesting aspects. The main objectives of this project are to reduce the mass of the Wheel Hub and therefore interesting to analyse and used in the Concept Screening.

Table 4.1. Comparative Design Analysis

 		
<p style="text-align: center;">Audi S1 EKS RX Ford Fiesta S2000/WRC Manufactured by Pankl System AG</p>		
Number of parts	5	1
Mass assembled Wheel Hub [g]	4776	2864
Advantages of design	Simple design (1). Used on the car today with desired function (2). CV-joint can be disassembled when the Wheel Hub is assembled on the car(3).	Manufactured in one piece (1). Compact design (2).
Disadvantages of design	Heavy (1).	Wheel Hub/upright need to be disassemble the to change CV-joint (2). Unable to change the Brake Disk easily (3).

4.2 Concept Screening

To fulfil the objectives to reduce the mass in the Wheel Hub, a method to re-design the Wheel Hub in terms of design and number of parts are performed. By comparing the current Wheel Hub with other designs on the market and the Pankl System-Wheel Hub. A simple CAD-model with only important properties of the parts are performed to make it easier to develop ideas that could be use later in the development phase. The choice of perform this work in CAD compared by drawings by hand was to be able to easy change the dimensions and put all parts together in an assembly to see the function, and dimensions in relations.

Figure 4.2 showing a concept where the Brake Disk Adapter is included in the Wheel Hub. Figure 4.3 shows a re-designed Socket that is made in another material to gain mass of the total unit. Figure 4.4 a very lighted version, the aim with this is to gain lower mass and all the design need to be tested carefully in the Finite Element Analysis-software and combined with the other concepts.

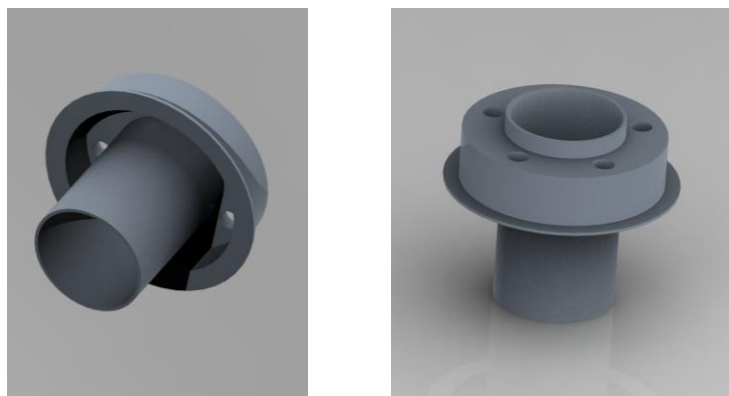


Figure 4.2. Concept Hub - 1

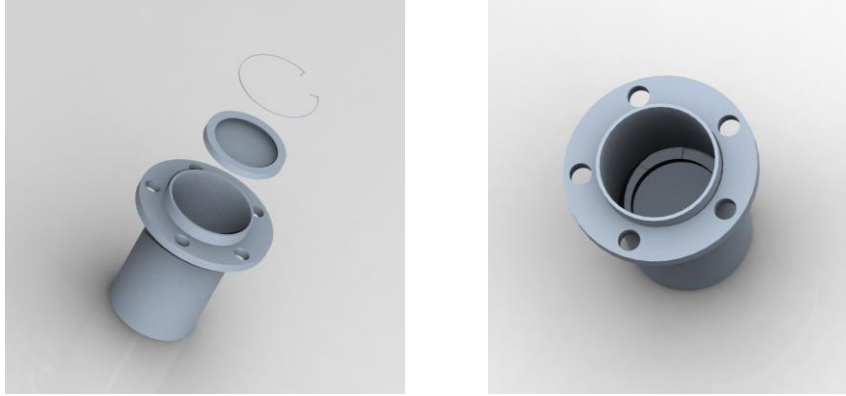


Figure 4.3. Concept Hub - 2

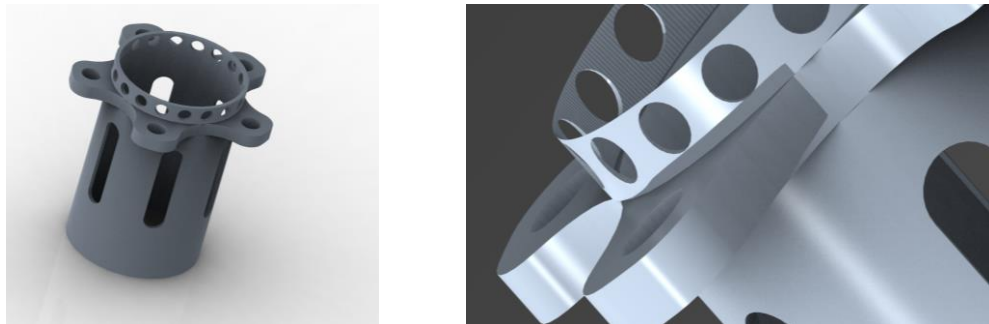


Figure 4.4. Concept Hub - 3

4.3 System Optimization

The designs are evaluated both as an assembly, and each part separately. This, to study an optimal design for the part but also the effects of the total assembly of the Wheel Hub. This is an iterative process and part by part is analysed, and the total gain in strength, mass and mechanical use-perspective. An algorithm used as; reduce material on parts that are affected by minor forces, re-design of important parts, optimization of critical parts that are affected by large forces within shape, size and topology are discussed (Vitthal Wable & Sanjong Shah, 2017).

4.4 Structural Optimization

The concepts from the Comparative Analysis, Concept Screening and System Optimization are now developed with CAE-software's where CAE are Computer Aided Engineering, to optimize the dimensions and geometry to effective the strength with respect to minimal mass. The concepts are analysed deeply and present by evaluation of reduced mass. Optimization of the current design is considered not enough improvements due to the design aspects, this is described in Section 4.12 and the complete new/re-designed Wheel Hub is described in the result part.

4.5 Terminology and Standard SAE J670

To make this project and analysis useful both in this project, but also in other applications in the vehicle dynamic analysis the standard ISO 8855:1991 is used. The terminology developed by *SAE International* and corresponding to the international standard of SAE J670 (SAE International, 2018). SAE International is a “*Global body of scientists, engineers, and practitioners that advances self-propelled vehicle and system knowledge in a neutral forum for the benefit of society*” (SAE International, 2018). The standard is limited to passenger cars with two axles and the standard recognizes axis system with both z-up and z-down orientation, but only z-up will be used in this thesis, see Figure 4.5. Axis system of three orthogonal directions with x, y and z. x-direction fixed in the vehicle travelling direction (Milliken & Milliken, 1997). A right-handed axis system is assumed (SAE

International, 2018). SAE J670 includes definitions for suspension, vehicle components and these will be used to the extent possible.

The vehicle dynamic of; roll, pitch and yaw are defined in Figure 4.5 from where:

- Roll, rotation about the x -axis
- Pitch, rotation about the y -axis
- Yaw, rotation about the z -axis

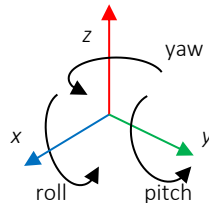


Figure 4.5. Coordinate System and roll, pitch, yaw - Definition

4.6 Definition of Sprung and Unsprung masses

This project is related to the unsprung parts of the suspension system and the sprung mass used in theoretical models and simulations only for evaluations. In the SAE J670-Standard, the sprung mass is defined as:

“All weight that is supported by the suspension, including portions of the weight of the suspension members. The sprung weight is the vehicle operating weight less the unsprung weight and the sprung mass is the sprung weight divided by the gravitational constant” (SAE International, 2018).

Further is the unsprung mass defined as:

“All weight that is not carried by the suspension but is supported directly by the tires. The unsprung weight includes the weight of the tires and wheels and all parts that move directly with the tires and wheels, plus a portion of the weight of the suspension linkages, ride springs, and driveshafts. The unsprung weight divided by the gravitational constant” (SAE International, 2018).

4.7 Theoretical and mathematical models

To describe physical and mechanical phenomena the theory of vibrations and behaviour of spring-mass systems is important and will be performed in a simplified way in this project. To make a complete analysis of the car regarding balance, mass distribution, performance etc. every section of the car is analysed in subsystems, which is a self-contained system within a larger system related to the total movement of the car. In this project time limits and computer software limitations makes it impossible to perform this type of analysis. To evaluate the behaviour and make an understanding of how the subsystem of the car, in this project the suspension is used with simplified models by paper and numerical software. Only academic and student licences of the software's can in some cases limit the possibilities of advanced systems, that makes it important to assume and analyse each part to make an accurate simulation. The theory, and mathematical relationships is the same for all applications. Example of this, the wheel will behave as a spring and damper due to the movement in the tire, therefore this need to be considered, or neglected depending on model. Tire damping is approximate 2% in the car and residual movement will be damped by the suspension (KAZ Technologies, 2018).

Further, the mass of the body work is considered due to the mass distribution.

If a model of a Quarter-Car is used, the mass can be assumed as 25% of the actual mass. This can be a good assumption, but also make the simulation incorrect if the assumption is wrong, due to the mass balance of the car.

System that is simplified can also consists of subsystems. The tire, or road input can in some cases be used as subsystems to make the modelling of the systems simpler. The outputs of this will then be added to the total system, and thus give very realistic simulation result of complex systems. How to model a mechanical system depending on the application, software and the knowledge of the system and in most cases a simplification is enough for an in this degree of problem.

4.7.1 Mass spring system of Quarter-Car Model

One, or more masses suspended with a system of springs, and dampers that is set in movement from input W . A 1D-system contains one mass, and a 2D-system contains two masses, a sprung mass m_s and an unsprung mass m_{us} (Anderson & Harty, 2010). In this project the 2D-system is relevant to use, because of the unsprung mass will be analysed. See Figure 4.6. The tire is modelled with a spring and a damper to simulate the movement and damping. The model in Figure 4.6 is used to make a simulation in MATLAB® and Simulink® (Messner & Tilbury, 2018).

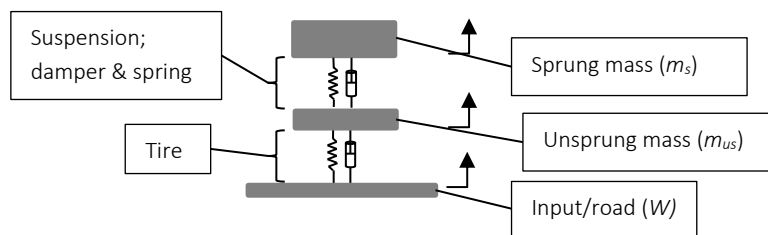


Figure 4.6. 2D-mass spring system

The input W can be either an impulse or an oscillated displacement. Once the masses are disturbed from the equilibrium, the position can be calculated and measured. Depending on the relations between the masses, springs, dampers and input the behaviour of the mass system can be analysed. The system can be analysed with a several aspects such; displacement, acceleration and velocity. The damper connected between the body work of the car (sprung mass) and the upright (unsprung mass) is used to control the movement of the masses (Dhakar & Ranjan, 2016). The spring in the system is used to hold the sprung mass at a specific height and to absorb bumps from the road input.

4.7.2 MATLAB® and Simulink® simulation

To make the importance of a low unsprung mass m_{us} , a model of a quarter car is performed in MATLAB® and Simulink®. In the model, a step W is modelled as a sinus curve or a step to evaluate, and visually show the position, acceleration and velocity of both sprung mass m_s and unsprung mass m_{us} . A step-simulation is shown in Figure 4.7. The tire model including Stiffness and Damping Coefficients is selected as default to; Tire Stiffness $1 \cdot 10^6$ N/m and Tire Damping 100 N/(m/s), (The Mathworks Inc, 2018). The suspension is modelled with a spring and a damper that is only selected with an arbitrary value to perform the behaviour of the system, this is changed depending on track, conditions and driving style. These parameters can be optimized with both unsprung masses explained but are neglected in this process. The simulation plotted in Figure 4.7 shows that the lower unsprung mass of 25 kg (green) responses on the bump quicker and has the possibilities to follow the track better compared to the larger unsprung mass of 35 kg (orange), both masses are arbitrary selected. The lower unsprung mass will result in a lower peak in movement and stop oscillate and come to a

stationary position faster. Minor differences in the sprung mass position, but in the theory explained in the Introduction, the traction is important, and the tire need to have contact with the surface.

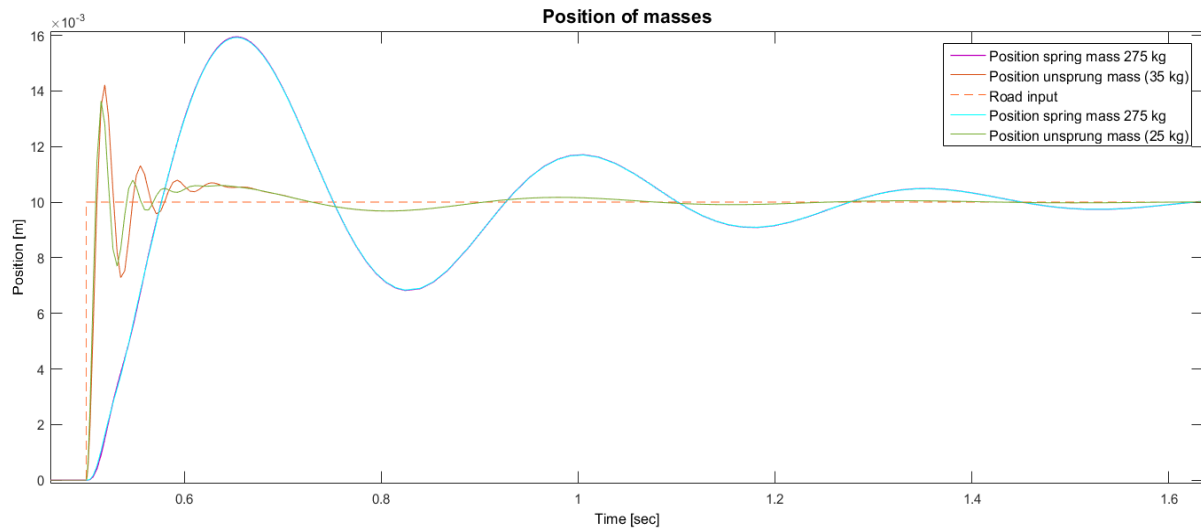


Figure 4.7. Simulation plot from Simulink of two different unsprung masses - Position

4.8 Materials

The material properties used in the analysis and conclusions is based on data collected from a third-party source, as material handbooks, material selection software's and resellers of the specific material. All data collected is controlled with different sources to verify that the data is correct. The material properties used in the simulations may differ from the material data from specific manufacturer, therefore are the conclusions and references performed on the materials given in this project. Further analysis and responsible of evaluating or compare this data is leaved to EKS. See Table 4.2 for properties of the materials discussed in this project (Aircraft Materials Ltd, 2018), (AZoM, 2018), (Dynamic Materials Ltd, 2018), (Sundström, 1998 (edit. 2013)). In this project, the material of the Wheel Hub is recommended by EKS (Ljungberg, 2018) to use the Steel 300M. The Steel 300M "offers a combination of toughness and ductility at high strength levels without an increased carbon content" (Aircraft Materials Ltd, 2018).

For chemical properties see Table 4.3 (Aircraft Materials Ltd, 2018), (AZoM, 2018), (Dynamic Materials Ltd, 2018), (Sundström, 1998 (edit. 2013)).

Table 4.2. Material Data (Aircraft Materials Ltd, 2018), (AZoM, 2018), (Dynamic Materials Ltd, 2018), (Sundström, 1998 (edit. 2013))

Mechanical Properties	Alloy 15CDV6, 17734.5	Steel C55 1.0535	Steel 300M	Aluminium 7075-T6
Tensile Strength [MPa]	980-1180	700-850	1980	572
Yield Strength [MPa]	790	450	1860	503
Elongation [%]	11	15	11	11
Hardness [HB]	293-352	-	520	150
Modulus of Elasticity [GPa]	205	210	205	71.5
Poisson's coefficient	0.3	0.3	0.28	0.33
Density [g/cm ³]	7.85	7.85	7.8	2.81
Thermal coefficient [1/°C]	1.18E-5	1.18E-5	2.32E-5	2.32E-5

Table 4.3. Chemical Properties of materials (Aircraft Materials Ltd, 2018), (AZoM, 2018), (Dynamic Materials Ltd, 2018), (Sundström, 1998 (edit. 2013))

Chemical composition [Wt %]	Alloy 15CDV6, 1.7734.5	Steel C55 1.0535	Steel 300M	Aluminium 7075-T6
C	0.12-0.18	0.52-0.6	0.40-0.46	-
P	<0.02	<0.045	-	-
Si	<0.2	<0.4	1.45-1.80	<0.4
V	0.2-0.3	-	0.05-0.10	-
Mn	0.08-1.1	0.6-0.9	0.65-0.90	<0.3
S	<0.015	<0.045	-	-
Mo	0.8-1	<0.1	-	-
Fe	Bal	-	-	<0.5
Al	-	-	-	87.1-91.4
Cr	-	<0.4	0.70-0.95	0.18-0.28
Cu	-	-	-	1.2-2
Mg	-	-	-	2.1-2.9
Ti	-	-	-	<0.2
Zn	-	-	-	5.1-6.1
Ni	-	-	1.65-2.00	-

4.8.1 Current Material used in Wheel Hub, Socket and Tap

4.8.1.1 Wheel Hub

The material used in the current Wheel Hub is High-Carbon Steel Alloy 15CDV6 number 1.7734.5 (Ljungberg, 2018). “Alloy 15CDV6 is steel which combines a high yield strength (superior to SAE 4130) with good toughness and weldability. This alloy finds many applications in the aerospace and motorsport industries in such components as roll cages, pressure vessels, suspension, rocket motors casings, wish bones and subframes” (Aircraft Materials Ltd, 2018). Material properties of Alloy 15CDV6 in Table 4.2 is from the properties specified at Aircraft Materials Ltd and from Dynamic Materials Ltd (Dynamic Materials Ltd, 2018).

4.8.1.2 Socket

The Socket is made in a Medium-Carbon Steel C55 1.0535 (Ljungberg, 2018). The Socket is only affected by the axial forces caused by the movement of the suspension and driveshaft during driving. By analysing the assembly of the part and discussions with EKS (Ljungberg, 2018), the axial forces are relative small. The material used in the current Socket is in that case over dimensioned. A reconstruction of the design and a change in material is performed to gain the unsprung mass. To obtain and evaluate design or material selections Creo is used to perform Finite Element Analysis of each concept. Cost of material and manufacturing is not considered in this project as not in the problem formulation from EKS (Ljungberg, 2018). Environmental aspects in the choice of material is considered as a request from University of Skövde. The selection of material is done with CES EduPack software to evaluate the environmental impact, and the Finite Element-simulation is to verify the function of the part. The calculations of Transport, Use and Disposal are neglected in the analysis. By analysing the loads and the function of the Socket, an idea to make a product of ABS plastic, after a further analysis of material properties no plastic compound that can withstand the heat generated from the brakes. Further, composite material is evaluated. The ceramic materials, that is manufactured by compressing particles into the desired shape is not that resistant for impacts that can occur. The analysis of material is focused to metals and alloys, and the Aluminium 7075-T6 is recommended and used by EKS previously (Ljungberg, 2018). A model is performed and EKS can decide the choice of manufacturing, due to the manufacturing techniques are neglected in this thesis.

4.8.1.3 Tap

The current Tap assembled in the CV-joint is manufactured in Aluminium 7075-T6. The shape of the part is very simple. An analyse of the Tap due to the mass is preformed, and the target is to machine the current part, therefore no material analysis of this part. A model is performed and EKS can decide the choice of manufacturing.

4.9 Calculation of acting loads

To perform relevant analysis of the Wheel Hub, an analysis of acting loads is performed. A decision to make the analysis in 2D, two dimensions is made to simplify the equations and making the equations solvable by hand and using a MATLAB®. The force-calculation on the Wheel Hub is performed in 2D to make it clear and easy to understand, a more complex model can be used but 2D is enough in this type of calculations (Genta, 1997).

4.9.1 Assumptions made in the calculations and Finite Element Analysis

In the calculations made to find acting loads, some assumptions are required. The friction coefficient between the tire and the road is set to “fixed”. This is done due to find the maximum force due to uncertainty of the friction coefficient between the rubber (tire) and asphalt. An example value of the friction coefficient is $\approx 0.5-0.8$ from (Engineeringtoolbox, 2018). Without a slip between the tire and road, the magnitude of the force reaches its maximum value, see Equation (4.1) and with a “fixed”-value assumption of the friction coefficient set to, $\mu=1$ and relation in Equation (4.2) is used. See also Equation (1.3) to get an idea of the assumptions made with respect to the friction-equation.

$$\frac{|F|}{|N|} < \mu \quad (4.1)$$

$$\text{With } \mu=1 \rightarrow |F| = |N| \quad (4.2)$$

The position of the *CGH*, Centre of Gravity and Moment of Inertia *I* (not calculated due to conclusion in 4.9.7) are in these calculations set to a fixed point, see conclusion developed in the data analysis in Section 4.9.3.

The attachment area of the rim to the Hub is set to cover the full area of the rim. The real case is that the rim only connects to smaller area around the wheel bolts. This assumption is made due to the simplification and that it not will affect the simulations in a negatively way.

4.9.2 Dimensions

The dimensions used to calculate the forces acting on the Wheel Hub is based on a standard Audi S1-car. The only parameter changed is the width for the rallycross car, an increased width of 140 mm from the standard car is given from EKS (Ljungberg, 2018). The assumption of the position relative to the ground, and coordinate system centred under the car is set as one third of the height *H* (Segers, 2014), see Table 4.4.

For constant data and vehicle parameters used in the calculations, see Table 4.4.

Table 4.4. Parameters for calculations of acting loads

	Parameter	Notation	Value	Unit
Mass	Total mass	M	1300	kg
	Unspung mass (1/4 of car)	m_{us}	30	kg
	Sprung mass (1/4 of car)	m_s	295	kg
Dimentions	Wheel base	Wb	2470	mm
	Width	Tw	1610 (1470+140)	mm
	Total height	H	1400	mm
	Centre of Gravity height	CGH	467	mm
	Centre of Gravity to left/right wheel	CG	805	mm
	Centre of Gravity to front axle	Lf	1235	mm
	Centre of Gravity to rear axle	Lr	1235	mm
	Wheel radius	Wr	350	mm
	Wheel width	Ww	250	mm
Engine	Torque from driveline	$T_{driveline}$	750-800	Nm

4.9.3 Data Analysis

Data collected from the car during a test at Circuit de Mayenne, France in 2017-08-28. Collected with Bosch WinDarab, a Data Management-software for analysing logged data from the sensors in the car. The software is not available to use in this project, a txt.-file with a sample of data is compiled and imported into MATLAB® for analysis.

Type of data collected:

- Time [sec]
- Acceleration in three dimensions x , y , z -directions [m/s^2]
- Clutch Pressure [Bar]
- Brake Pressure, Front and Rear axle [Bar]
- Damper Positions [mm]
- Steering Angle [°]
- Speed [m/s]

Information of movement in chassis are not collected from the car. This information can be calculated as a mathematical channel from the damper sensors. The damper positions are calibrated with respect to the position when the car stands at rest. A negative (<0) value represents a compression of the damper, and the positive value (>0) an extension (Segers, 2014). With this data, the movement of the chassis can be calculated. The damper position data collected are plotted with MATLAB® into a graph, see Figure 4.8 for each wheel of the car.

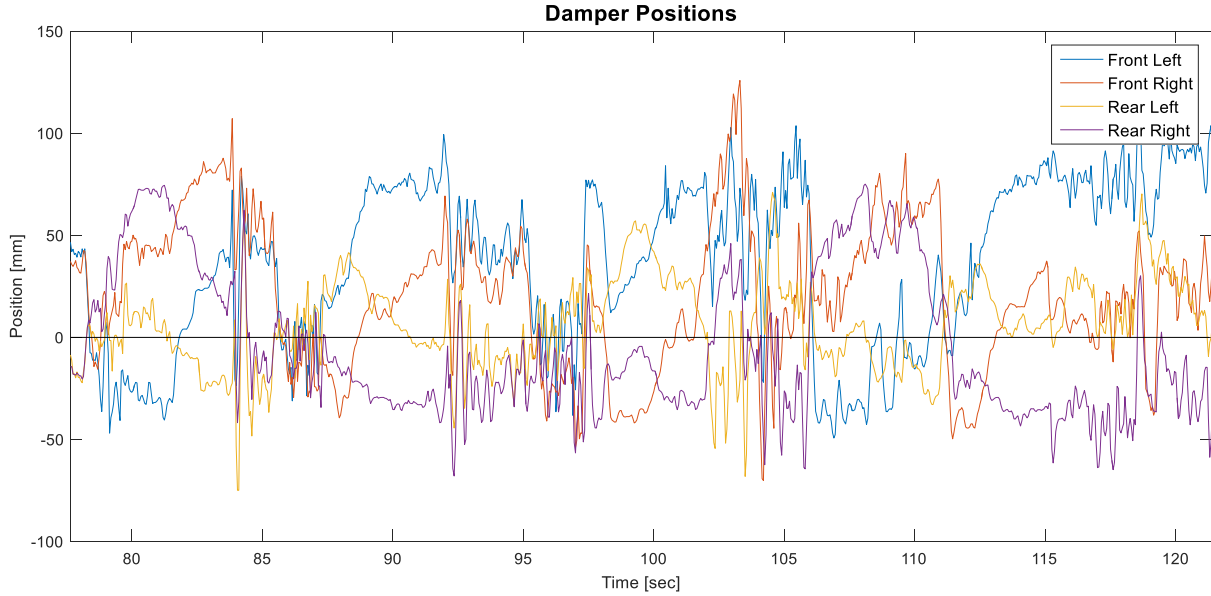


Figure 4.8. Damper positions

The relations between the left and right-side dampers can represent the roll angle θ , and the relations between the mean of the front and rear dampers represents the pitch angle Φ , see Equation (4.3), (4.4) and (4.5) which are derived in Analysis techniques for racecar data acquisition and used in this project (Segers, 2014). A plot with MATLAB® is performed to find the mean values of the damper positions collected, see Figure 4.9.

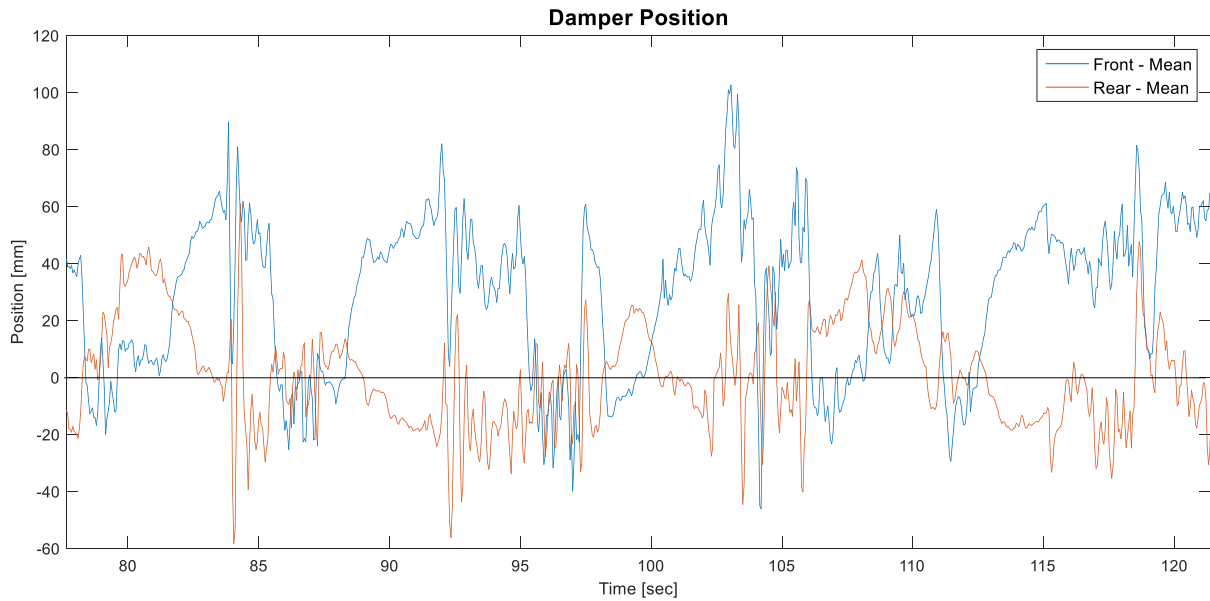


Figure 4.9. Damper position - mean front and rear

The roll and pitch angles, defined in Figure 4.5 are interesting in that way of; the mass transfer, change in position for the Centre of Gravity in the car. This analysis is performed in a way that answer the questions if the information is relevant in the calculations of forces acting on the Wheel Hub. Equations where z is the damper positions with index of the location on the car, T_w is the width of the car and W_b the Wheel base. For numerical data see Table 4.4 and Figure 4.8 for the values used.

$$\text{Roll angle } \theta \text{ (Rear Axle)} = \tan^{-1} \left[\frac{z_{RL} - z_{RR}}{T_w} \right] \quad (4.3)$$

$$\text{Roll angle } \theta \text{ (Total)} = \tan^{-1} \left[\frac{(z_{FL} - z_{FR}) + (z_{RL} - z_{RR})}{2Tw} \right] \quad (4.4)$$

The pitch angle using Equation (4.5):

$$\text{Pitch angle } \Phi \text{ (Total)} = \tan^{-1} \left[\frac{z_F - z_R}{Wb} \right] \quad (4.5)$$

The movement for the chassis in roll and pitch from Equations (4.3), (4.4), (4.5) (Segers, 2014) and result in plotted graphs with MATLAB® in Figure 4.10.

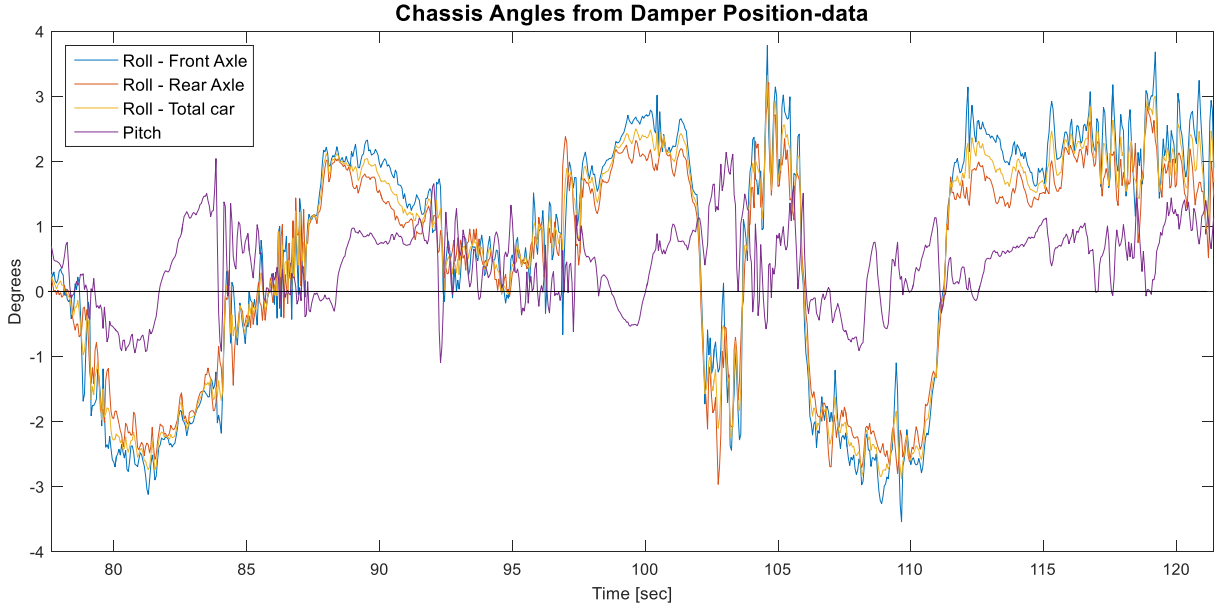


Figure 4.10. Roll and pitch from data analysis

The angles of the chassis (pitch and roll) are small in normal driving, about $\pm 3^\circ$. Yaw angle not affect the position of Centre of Gravity due to rotation only in the x - y -plane. The change in position for Centre of Gravity due to the pitch and roll gives in Equations (4.6) and (4.7) a position change of approximate ± 24.4 mm, see Figure 4.11. The change in position of the Centre of Gravity is therefore assumed to not affect the calculations of forces in the Wheel Hub. A conclusion with EKS (Ljungberg, 2018) and discussed in that these small changes can be neglected (Jiang, Pavelescu, Correa Victorino, & Ali, 2014), (Segers, 2014). The vertical dotted-line in Figure 4.11 represents the initial position for the Centre of Gravity.

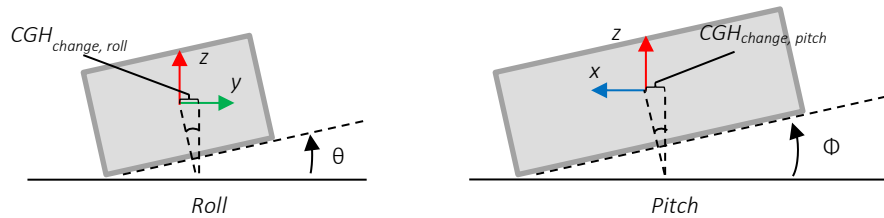


Figure 4.11. Centre of Gravity change in position

$$CGH_{change,roll} = CGH \sin \theta \quad (4.6)$$

$$CGH_{change,pitch} = CGH \sin \Phi \quad (4.7)$$

4.9.4 Forces - Normal conditions

To calculate the forces on the wheels, two Free Body Diagrams are performed in Figure 4.12 the car is seen from the front, and Figure 4.13 the car is seen from the left side to make assumptions of the forces acting. A “Normal condition”-drive is where no un-normal behaviour of the car appears, and the track is smooth with no ruts, wet or loose gravel and tarmac.

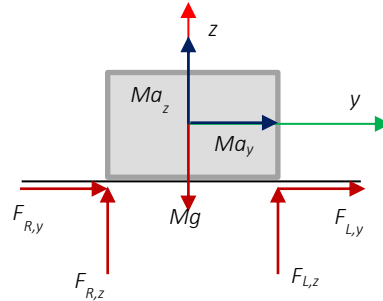


Figure 4.12. Free Body Diagram y-z-plane

The Equations (4.8) and (4.9) in y-z-plane, car observed from the front in Figure 4.12 yields:

$$y^{\rightarrow}: F_{R,y} + F_{L,y} = Ma_y \quad (4.8)$$

$$z^{\uparrow}: F_{R,z} + F_{L,z} - Mg = Ma_z \quad (4.9)$$

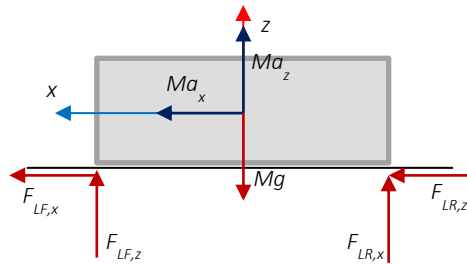


Figure 4.13. Free Body Diagram x-z-plane

The Equations (4.10) and (4.11) in x-z-plane, car observed from the left in Figure 4.13 yields:

$$x^{\leftarrow}: F_{LF,x} + F_{LR,x} = Ma_x \quad (4.10)$$

$$z^{\uparrow}: F_{LF,z} + F_{LR,z} - Mg = Ma_z \quad (4.11)$$

Equation (4.8) to (4.11) satisfies the forces in the Hub only in the region with fully developed friction, see Equation (4.1). With variation and unknown of the friction coefficient μ , and the maximum forces are interesting, the friction coefficient is set to $\mu=1$. Therefore, the forces acting on the wheel is equal ($F_{LR,x}=F_{LF,x}$, $F_{LR,z}=F_{LF,z}$, $F_{L,y}=F_{R,y}$, $F_{L,z}=F_{R,z}$) to the mass times the acceleration. By the symmetry of the car and assumptions made the $F_{LR,x}=F_{LF,x}=F_x$, $F_{L,y}=F_{R,y}=F_y$ and $F_{LR,z}=F_{LF,z}=F_z$. These forces are calculated to an approximate value of ± 3000 N for F_x (blue) and F_y (orange). Force in the z-direction F_z (green) yield an approximate value of ± 15000 N and a plot of this is performed in Figure 4.14.

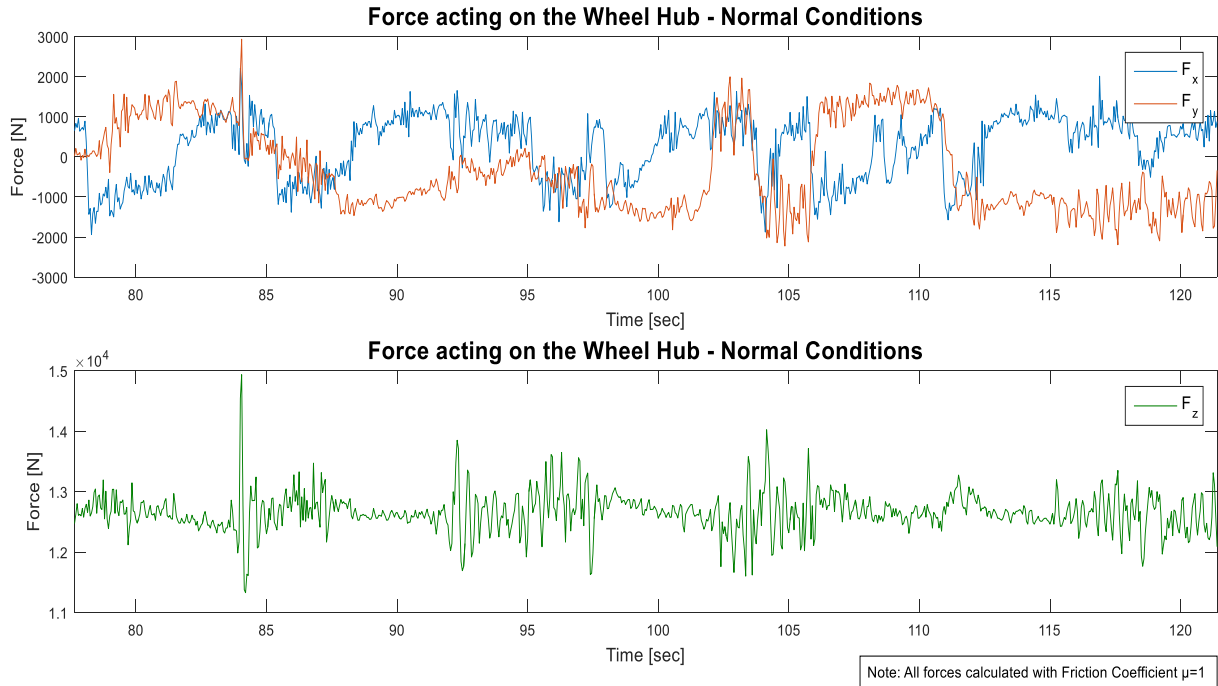


Figure 4.14. Forces normal conditions

To assume and show that the forces acting on the ground is equal or assumed to be equal at the Hub see Figure 4.15. By static Equations (4.12) and (4.13) the forces on the system are in equilibrium when the forces at the ground are equal to the forces at the Hub. This assumption will be use in this project as a simplification, some differences will be covered by a Safety Factor.

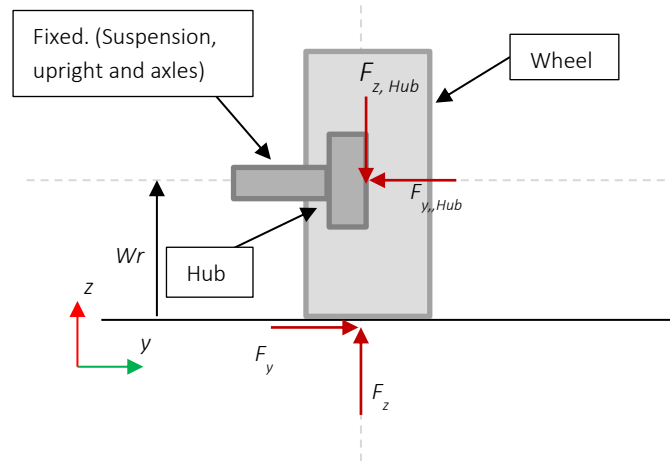


Figure 4.15. Forces on Hub and wheel

$$y^{\rightarrow}: F_y - F_{y,Hub} = 0 \quad (4.12)$$

$$z^{\uparrow}: F_z - F_{z,Hub} = 0 \quad (4.13)$$

4.9.5 Acceleration torque

From the given output the torque from engine and gearbox is $T_{driveline} \approx 750-800$ Nm according to information given by EKS (Ljungberg, 2018). With the assumption of maximum friction, gives that the torque applied to the Wheel Hub is in the same region, see Figure 4.16.

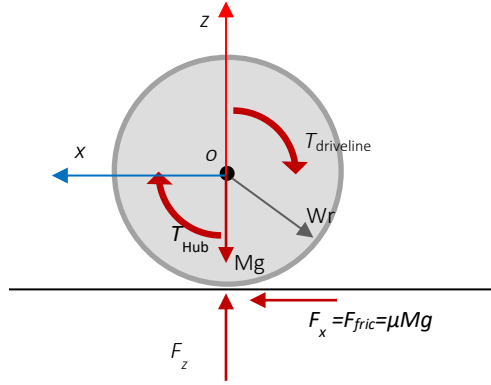


Figure 4.16. Free Body Diagram Torque applied

Equilibrium from Free Body Diagram in Figure 4.16 gives Equation (4.14):

$$M_O^{\circ} = T_{drive} + T_{Hub} + \mu N W r = 0 \quad (4.14)$$

With the assumption of no slip, gives a torque on the Hub approximate $T_{Hub} \approx 314 \text{ Nm}$.

4.9.6 Braking torque

The Wheel Hub is affected through the Brake Disk Adapter which is assembled on the Hub and fixed on the wheel nuts with the rim (Sharma & Nain, 2015). The moment acting on the Hub is interesting. Things that has to be consider when making assumptions of this is the Brake Balance, the speed and acceleration of the car. These data are collected and used in this analysis, see Figure 4.17 for a plot of Speed vs. time in MATLAB® from the collected data. The Brake Pressure, or Brake Balance is not analysed, and the braking is only calculated related to the total acceleration during the braking.

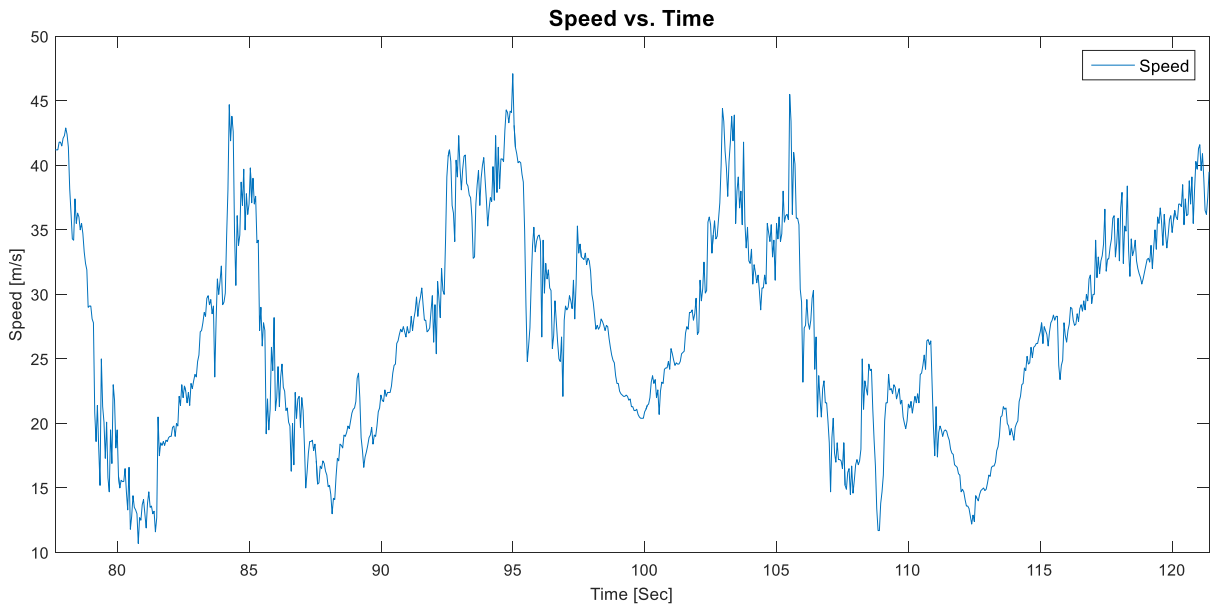


Figure 4.17. Speed vs. Time

The maximum acceleration during a braking, see Equation (4.15) (Segers, 2014), (Jansson & Grahn, 2013) which also showing the definition of acceleration with respect of time. The highest acceleration $a_{braking}$ with Equation (4.15) and analysis of Figure 4.17 is -30 m/s^2 .

$$a_{braking} = \frac{\Delta speed}{\Delta time} = \frac{18.60 - 35.40}{79.20 - 78.65} \quad (4.15)$$

The Free Body Diagram in Figure 4.18 showing the torque acting on the Wheel Hub and the forces from the ground during the braking, assumption this is equal at all four wheels and this calculation performed at the front, or rear right wheel. The Equation in (4.16) (Segers, 2014) gives a braking force of $F_{braking} \approx -9927$ N. Equation (4.16) used in (4.17) (Segers, 2014) gives a braking torque applied of $T_{Hub, braking} \approx -3475$ Nm.

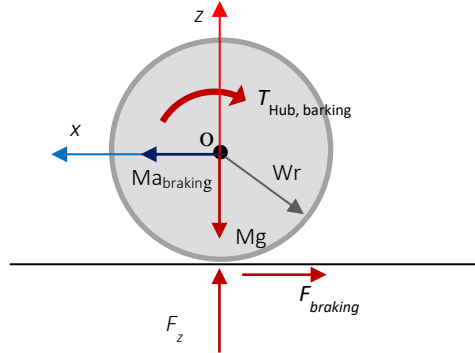


Figure 4.18. Free Body Diagram Braking

$$x^{\leftarrow}: -F_{braking} = Ma_{braking} \quad (4.16)$$

$$M_O^{\cup} = T_{Hub,braking} - WrF_{braking} = 0 \quad (4.17)$$

By comparing the torque applied in acceleration and the torque caused by the braking is approximate a factor of ten larger, and therefore the most critical torque acting on the Hub.

4.9.7 Forces - Impact forces and Special cases

Forces acting on the car, tires and Wheel Hub in normal use are given in Equations (4.8) to (4.17). To perform a more complex analysis of the Wheel Hub, a special case of forces is considered - impacts. Both impact from other competitors, but also while the car landing after a jump or hit a bump on the track. These cases are hard to simulate, and the assumptions are made. The forces developed in these calculations will not be dimensioning for the Hub, only used for evaluation. The forces occur on the Wheel Hub and car, may result in a failure of either the Wheel Hub or other suspension parts, so this analysis are only taken in account to analyse the behaviour of the Wheel Hub in extreme cases. The acceleration-data are measured in the fixed coordinate system in the car, and thus needed to be rotated to the coordinate system at the ground with a Rotation matrix \bar{R} , see Equation (4.18). The yaw angle γ , the defined angle represents the rotation about the z -axis of the car, Figure 4.5. In the analysis of normal condition, the chassis angles are neglected due to that the yaw does not count in the x - z and y - z -plane and roll and pitch are assumed as small, $\pm 3^\circ$. In this special case, the three chassis angles are assumed to represent a “worst case” scenario of an impact.

$$\bar{R} = \begin{bmatrix} (\cos \gamma \cos \theta) & (-\cos \gamma \sin \theta) & (\sin \gamma) \\ (\sin \Phi \sin \gamma \cos \theta + \cos \Phi \sin \gamma) & (-\sin \Phi \sin \gamma \sin \theta + \cos \Phi \cos \theta) & (-\sin \Phi \cos \theta) \\ (-\cos \Phi \sin \gamma \cos \theta + \sin \Phi \sin \theta) & (\cos \Phi \sin \gamma \sin \theta + \sin \Phi \cos \theta) & (\cos \Phi \cos \gamma) \end{bmatrix} \quad (4.18)$$

In Figure 4.19 the case studied is presented. No measured data from experiment or runs are used. An assumption of chassis angles is used to calculate the forces at one wheel, in this case the right front wheel. But the theory is the same for all four wheels. The suspension and tire are assumed as stiff and not changing the position. This study is to determine the maximum force, and this will be achieved with this assumption of rigid parts in the suspension.

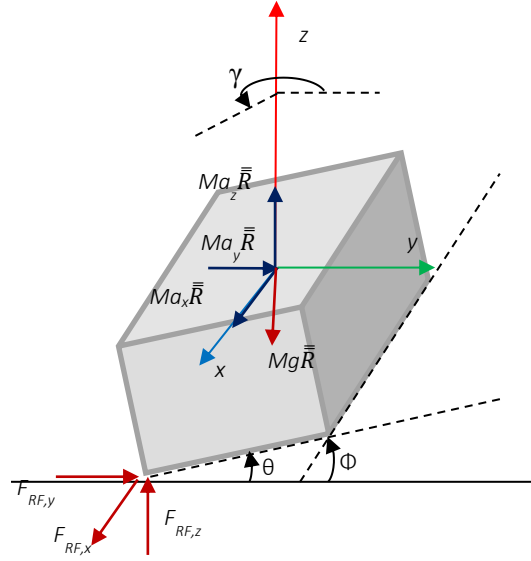


Figure 4.19. Forces acting on the car at one wheel

Equations (4.19), (4.20), (4.21), (4.22), (4.23), (4.24) based on Figure 4.19 in three dimensions.

$$x^{\leftarrow}: F_{RF,x} + Mg\bar{R} = Ma_x\bar{R} \quad (4.19)$$

$$y^{\rightarrow}: F_{RF,y} + Mg\bar{R} = Ma_y\bar{R} \quad (4.20)$$

$$z^{\uparrow}: F_{RF,z} + Mg\bar{R} = Ma_z\bar{R} \quad (4.21)$$

$$M_x^{\zeta} = \frac{Tw}{2} F_{RF,z}\bar{R} + CGH F_{RF,y}\bar{R} = I\alpha_{roll} \quad (4.22)$$

$$M_y^{\zeta} = \frac{Wb}{2} F_{RF,z}\bar{R} - CGH F_{RF,x}\bar{R} = I\alpha_{pitch} \quad (4.23)$$

$$M_z^{\zeta} = \frac{Wb}{2} F_{RF,y}\bar{R} + \frac{Tw}{2} F_{RF,x}\bar{R} = I\alpha_{yaw} \quad (4.24)$$

The accelerations in x , y , z -directions and the angular accelerations of roll, pitch and yaw acting on the car. A negative value of the accelerations represents that the car slows down in the landing. These values are only an assumption and used to find a critical case, this may not be a realistic case. No gyroscope or acceleration data in this case is provided and all data need to assume. By assuming accelerations a_x , a_y , a_z , angular accelerations α_{roll} , α_{pitch} , α_{yaw} and the angles of roll θ , pitch Φ and yaw γ the values of the forces $F_{RF,x}$, $F_{RF,y}$, $F_{RF,z}$ may not be as accurate as desired. This conclusion is made after discussion with Stefan Karlsson, Associate Professor in mathematics, Department of Engineering Science at University of Skövde. Due to this, the normal condition forces will be used, with an applied Safety Factor to cover the special cases of forces. Therefore, a more detailed analysis to select the Safety Factor is made in Section 4.10.

4.9.8 Heat load

The Wheel Hub and other parts is closely located to the Brake Disk. The Brake Disk can reach high temperatures and the CV-joint reaches 120°C from data given by EKS (Ljungberg, 2018). The heat expansion of the parts is an interesting, and important step in the optimization especially of the Wheel Hub. An assumption is made with EKS (Ljungberg, 2018) that the Wheel Hub can reach a temperature of at least 120°C, and this value will be used in the simulations, see Table 4.6.

4.10 Safety Factor

The Safety Factor due to the uncertainties in both the material properties, calculations of forces and load cases but also for the simplifications made in the analysis. The data properties used in the Finite Element Analysis are used from the specified material in the parts, and the properties are taken from manufacturer of each material.

The literature study did not reveal any generally used Safety Factor in the motorsport industry and therefore, a Safety Factor in the project is designed specific for this study.

To design a Safety Factor, the method used in Mechanical Design of Machine Elements and Machines (Collins, Busby, & Staab, 2010) is used. The steps described are picked from the book and cited in this thesis. The authors of the book (Collins, Busby, & Staab, 2010) select the safety factor based on, first consider each “rating factors” separately.

- 1) *The accuracy with which the loads, forces, deflections can be determined.*
- 2) *The accuracy with which stresses and or other loading parameters can be determined.*
- 3) *The accuracy with which the material properties can be determined*
- 4) *Need to conserve material, weight, space or money*
- 5) *Consequences of failure in terms of human life and/or property damage.*
- 6) *The quality of workmanship in manufacture.*
- 7) *The condition of operation.*
- 8) *The quality inspection and maintenance during operation.*

These factors are rated from Rating Number (RN) = -4 to 4, where each number represents as;

RN = 1	<i>“mild need to modify”</i>
RN = 2	<i>“moderate need to modify”</i>
RN = 3	<i>“strong need to modify”</i>
RN = 4	<i>“extreme need to modify”</i>

A positive (+) sign of Rating Number means that the factor need to increase the Safety Factor, and the number represent the importance (0 to 4). Negative sign (-) represent the need of decrease the Safety Factor needed. The value of RN is then used in Equation (4.25) to calculate s the sum of RN (Collins, Busby, & Staab, 2010).

$$s = \sum_{i=1}^8 (RN)_i \quad (4.25)$$

The Safety Factor SF is calculated by using Equation (4.26). This equation is satisfied for $s \geq -6$, for $s < -6$ gives directly $SF=1.25$ (Collins, Busby, & Staab, 2010).

$$SF = 1 + \frac{(10 + s)^2}{100} \quad (4.26)$$

By using Equations (4.25), (4.26) and a carefully considered RN gives $s=-2$, see Table 4.5. The Rating Numbers selected are based on assumptions made of the accuracy of the factors. Presented in Table 4.5 factors related to loads (factor 1 and 2) are rated high since it need to increase the Safety Factor, and factors of manufacturing (factor 7, 8 and 9) and need to conserve material are rated with a low Rating Number to reduce the Safety Factor.

Table 4.5. Rating Number and sum of RN

Factor #	1	2	3	4	5	6	7	8	Sum
Rating Number (RN)	4	3	1	-4	-2	-4	4	-4	-2

Using Table 4.5 and Equation (4.26) the Safety Factor is calculated to $SF=1.64$. By using Equation (4.27) the dimensioning force (general described) to be used in the simulation is calculated (Collins, Busby, & Staab, 2010).

$$F_n^{SF} = F_{calculated}SF \quad (4.27)$$

4.11 Finite Element Analysis and Optimization

The Finite Element Analysis is used to analyse the parts behaviour when a load is applied. The loads and conditions used as a base of the analysis performed comes from the pre-study, theoretical calculations and discussions with supervisor Ulf Stigh and EKS (Ljungberg, 2018). The vehicle dynamics used in the calculation of forces are now applied in a static analysis (Sajjan, Parthasarathy, Kiran P, & Kumar K N, 2016). The simulations are performed with solid three dimensional-models and triangular elements or, “tetrahedral”, see Figure 4.20 are used due to the geometrical small radius and sharp edges in the models.

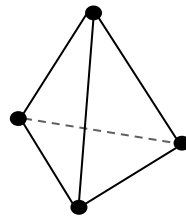


Figure 4.20. Tetrahedral element

The AutoGEM-tool for automatic generating of element mesh in Creo is used, and the settings are controlled to an accurate setup to the model. The meshes are presented in Figure 4.21 for the Hub and Figure 4.22 for the Cup. The p-method is used in Creo and allows a larger meshing of the parts. The convergence is set to 10% of the overall von Mises stresses, and is reached in all the simulations.

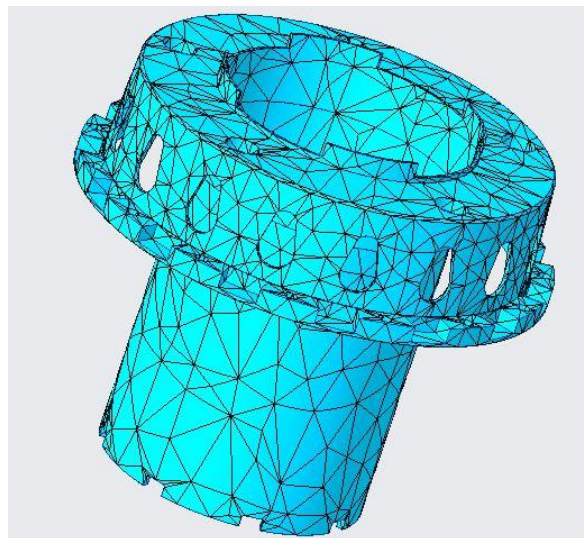


Figure 4.21. Tetrahedral elements mesh - Hub

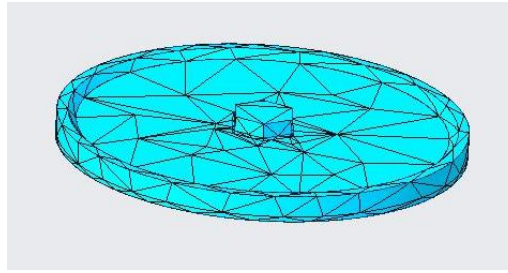


Figure 4.22. Tetrahedral elements mesh - Cup

4.11.1 Loads used in the Finite Element Analysis

The forces from theoretical and mathematical analysis of the Wheel Hub, combined with the Safety Factor calculated in Equation (4.27) is used as loads in the Finite Element Analysis, see Table 4.6.

Table 4.6. Dimensioning forces and torques

Force/load at one Wheel Hub	Calculated [N]	Safety Factor	Dimensioning force [N]
Force_x	3000	1.64	4920
Force_y	3000	1.64	4920
Force_z	15000	1.64	24600
Torque/load at one Wheel Hub	Calculated [Nm]	Safety Factor	Dimensioning force [Nm]
Torque_driveline	800	1.64	1312
Torque_braking	3475	1.64	5699
Force/load Socket	Assumed [N]	Safety Factor	Dimensioning force [N]
Force axial	400	1.64	656
Force radial	0	1.64	0
Force/load Tap	Assumed [N]	Safety Factor	Dimensioning force [N]
Force axial	400	1.64	656
Force radial	0	1.64	0
Force/load Cup	Assumed [N]	Safety Factor	Dimensioning force [N]
Force axial	400	1.64	656
Force radial	0	1.64	0
Heat load All parts	Assumed [°C]	Safety Factor	Dimensioning force [°C]
Heat rise	120	1.64	196.8

4.11.2 Finite Element Analysis of Wheel Hub - Current design

The current Wheel Hub from the given STEP-file from EKS is analysed with the specified material Alloy 15CDV6 and applied with the loads calculated, see Table 4.6. This job is done to evaluate the boundary conditions and that the current part can withstand the loads. If the Hub does not pass this analysis, the simulation or calculation need to be adjusted. No damages on the real Hub has occurred during the use at the car in races or testing during the past four years as information from EKS (Ljungberg, 2018).

The analysis in Figure 4.23 show that the current Hub withstands the loads without the heat with a factor of approximate two under the yield strength, see Table 4.2. Figure 4.24 shows the simulation with the heat load of 196.8°C applied on the Hub, and the Hub withstand also this case clearly below the yield strength if neglect the singularities that appears in the simulation. The data collected from EKS (Ljungberg, 2018), calculations and simulations in this analysis performed to prove the

assumptions in loading cases and boundary conditions used in all simulations of the Wheel Hub. The Wheel Hub are analysed with forces acting in x , y , z -direction on the flat surface that is fitted tight to the rim. A moment is applied at the interference point from the Brake Disk. The Hub is constrained with a pin-connection to simulate the bearing and fixed in the upright. A fully constrained region simulates the CV-joint. This is used as fixed to simulate the extreme value at the Hub and used also when analysing the re-designed Hub, see Section 4.12.1.1.

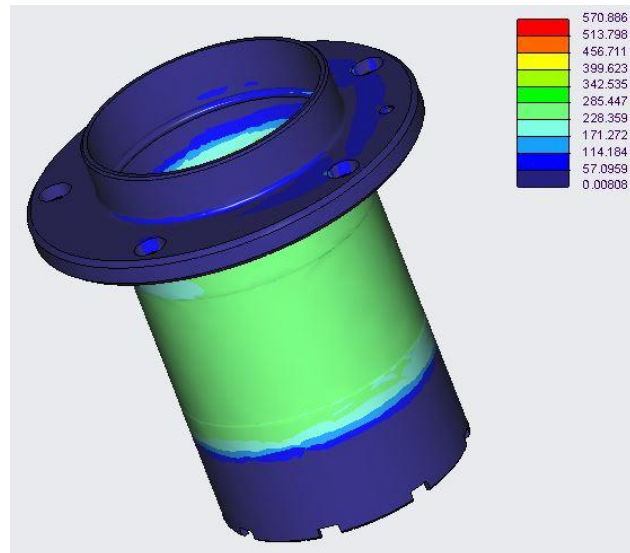


Figure 4.23. von Mises stresses in current Hub [MPa]

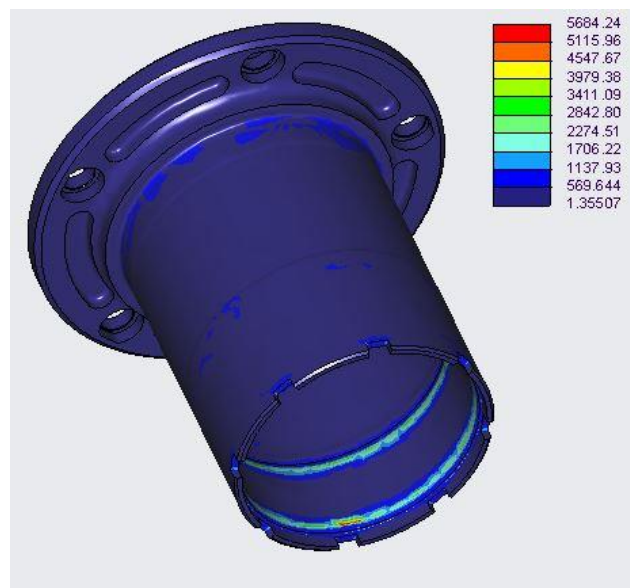


Figure 4.24. von Mises stresses in current Hub with heat load [MPa]

4.11.3 Finite Element Analysis of Brake Disk Adapter - Current design

As with the Wheel Hub, an analysis on the current Brake Disk Adapter to evaluate the simulation on the current part now working proper on the car. Moment from the Brake Disk is applied in the interfaces and the Adapter is fixed at the attachment surface to the Hub. In Figure 4.25 the stresses with the braking torque and heat load in Table 4.6 applied. The Adapter is manufactured in Aluminium 7075-T6 and this is used with the properties in Table 4.2. Figure 4.25 shows that the Adapter withstands the loads if singularities are neglected.

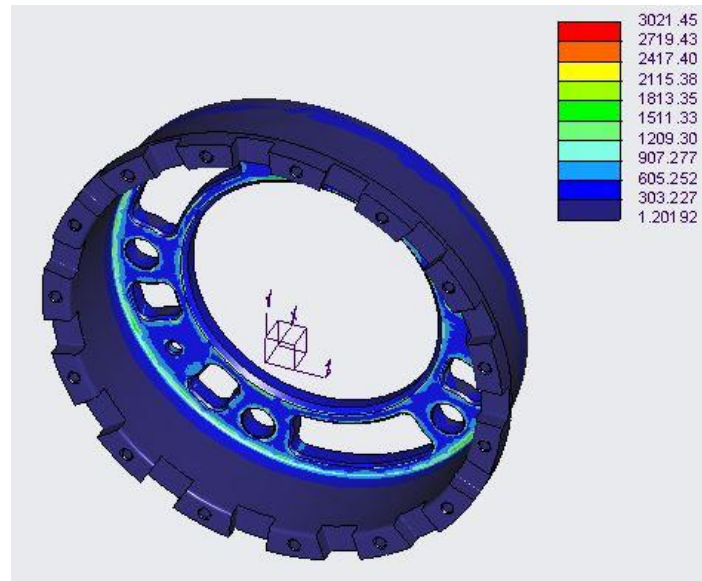


Figure 4.25. von Mises stresses in Current Brake Disk Adapter [MPa]

4.11.4 Finite Element Analysis of Socket - Current design

The current Socket is analysed with the current material Steel C55 1.0535, see Table 4.2 and applied with the axial loads in Table 4.6. The Socket is set as a pin-connection and is only able to deform in axial direction. The stresses appear in the part is shown in Figure 4.26.

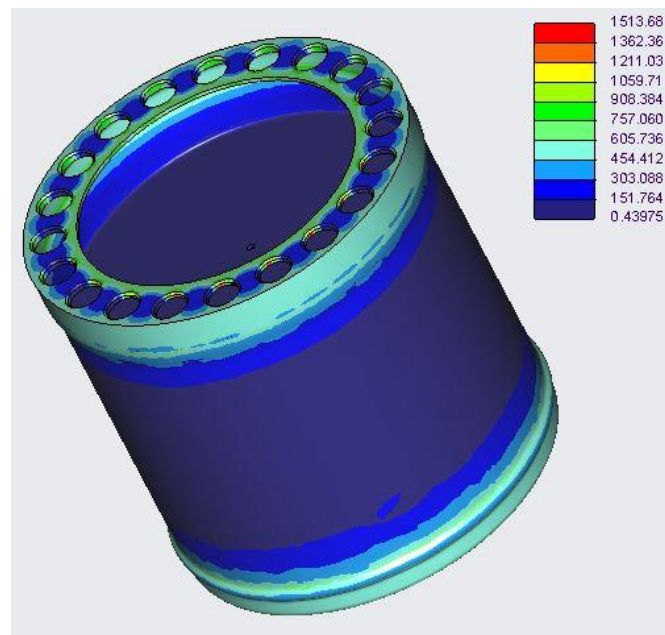


Figure 4.26. von Mises stresses in current Socket [MPa]

4.12 Design Analysis of the current Hub and Brake Disk Adapter

In the design analysis of the current Hub and with discussions with EKS (Ljungberg, 2018) there are relatively small changes that can be performed on the current Hub. The backside of the rim attachment can be modified, see Figure 4.27. This area could be modified on the four equal zones on the Hub but only reduce the mass of approximate 70 grams per Hub, see Table 5.1.



Figure 4.27. Wheel Hub backside of rim attachment area

The centring ring in Figure 4.28 on the Hub could be modified with a thinner wall, number 1 and the height from attachment surface for the rim, number 2.

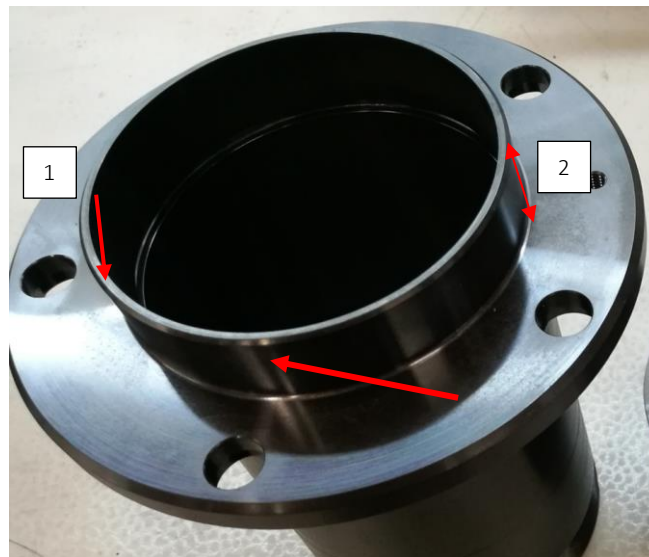


Figure 4.28. Hub centring ring

The Brake Disk Adapter used today on the car in Figure 4.29. Seen in that figure, the design is optimized with respect to the mass to the racing season 2018. Compared to the previous Adapter from 2017 in Figure 4.30 the decision to not put further development in the Adapter is made. No comparing analysis is performed in this stage, and this conclusion is made by visually analyse the two designs together with Janne Ljungberg at EKS (Ljungberg, 2018).

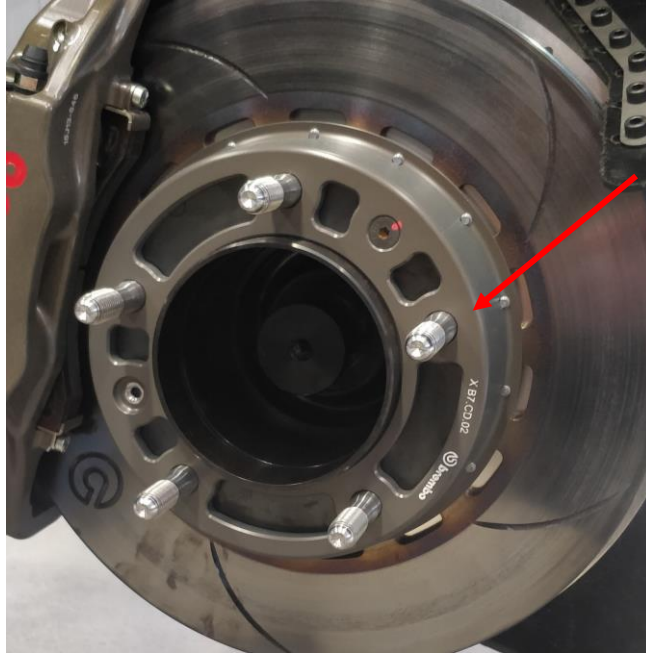


Figure 4.29. Current Brake Disk Adapter on the car 2018



Figure 4.30. Brake Disk Adapter 2017

4.12.1 Finite Element Analysis, Re-design and Optimization of the new Hub

From the ideas in the Concept Screening a Hub with the Brake Disk Adapter integrated. The Optimization-tool in Creo is used. The design is briefly discussed in the result, Section 5 in the thesis, but the design is presented in Figure 4.31 to make the Finite Element Analysis clear about the re-designed Wheel Hub. The full detailed re-designed Hub is presented in the result with explanations of the function.

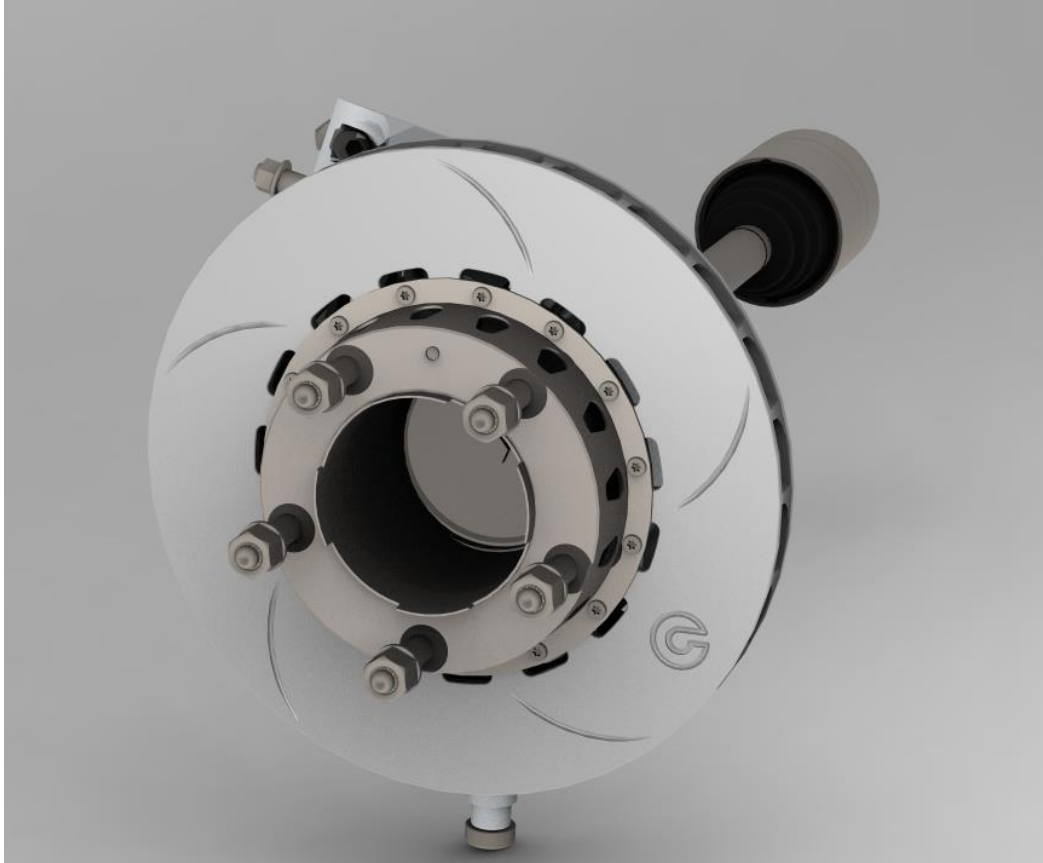


Figure 4.31. Re-designed Wheel Hub - Assembly

4.12.1.1 Boundary Conditions

The Boundary Conditions used in the Hub are presented in Figure 4.32. The attachment surface for the rim numbered 1 loaded by forces caused by the rim and calculated in Section 4.9, and the magnitude are presented in Table 4.6. The Wheel Hub is affected by a temperature-change and simulated by a heat load number 2. This heat load will not affect the simulation of the Hub alone and is used to analyse the different types of material, magnitude of the heat load, see Table 4.6. The Hub is supported by bearings and assembled inside the upright (not included in this project) and due to this be fixed in radial direction, free in axial and free to rotate, number 3. The area that interfaces the CV-joint and shown with blue/purple stars and numbered 4 in the figure is set to fixed displacement. Solid elements are used and therefore the rotational-freedoms are set to free, due to the solid elements characteristics. A moment caused by the braking moment and Brake Disk are applied at all interfaces pointing in rotation about centre axle of the Hub, number 5. A reference point in the centre of the Hub is selected as rotation point. The moment is applied as presented in Figure 4.32 due to the floating Brake Disk, for description of “floating disk” see Section 5.4.

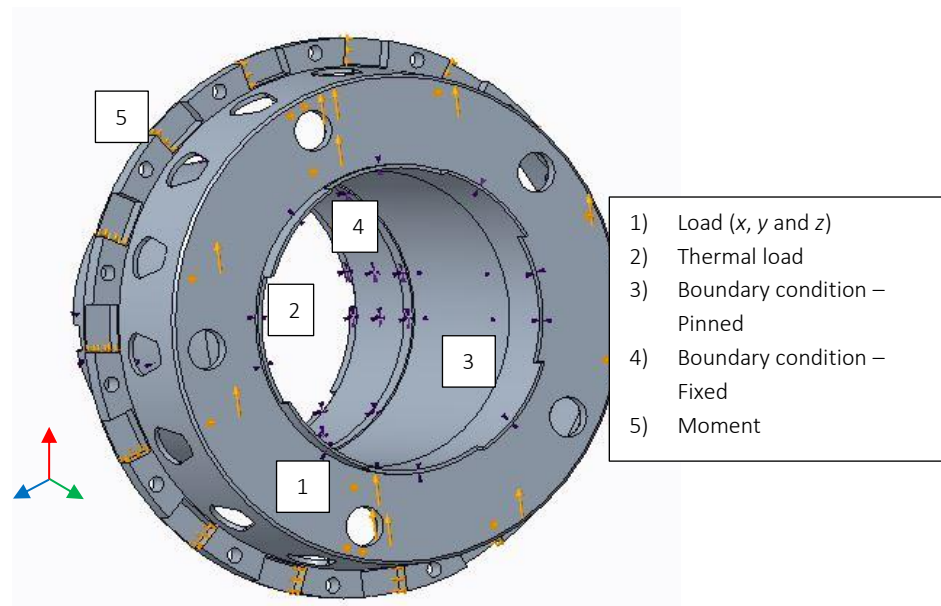


Figure 4.32. Boundary Conditions - Hub

4.12.1.2 Optimization work

The optimization of the Hub is performed on the regions marked green in Figure 4.33 with respect to mass vs. Von Mises stress of the yield strength in the material. The oval shaped holes both reduces the mass without lose in strength and works as ventilation of the Hub (no analyse with CFD, Computer Fluid Dynamics-simulations performed), number 1. The dimensions and geometry of the holes are set at parameters and used to find optimal shape. The areas affected by large moments the wall thickness is optimized and critically investigated. The upper green marked area, number 3 is the centring ring of the rim and is not affected by any large forces and the optimization in this area is performed to optimize the mass with retained function and required strength. The attachment surface for the rim need to carry the full load calculated in Section 4.9, see Figure 4.12. The thickness and design modifications green marked in Figure 4.33, number 2. The interfaces for the wheel nuts is fixed and used as in the current Hub to fit the rims. The iterative work to find an optimal design of the described sections and areas are performed. The selected dimensions and design are presented in the Section 5.

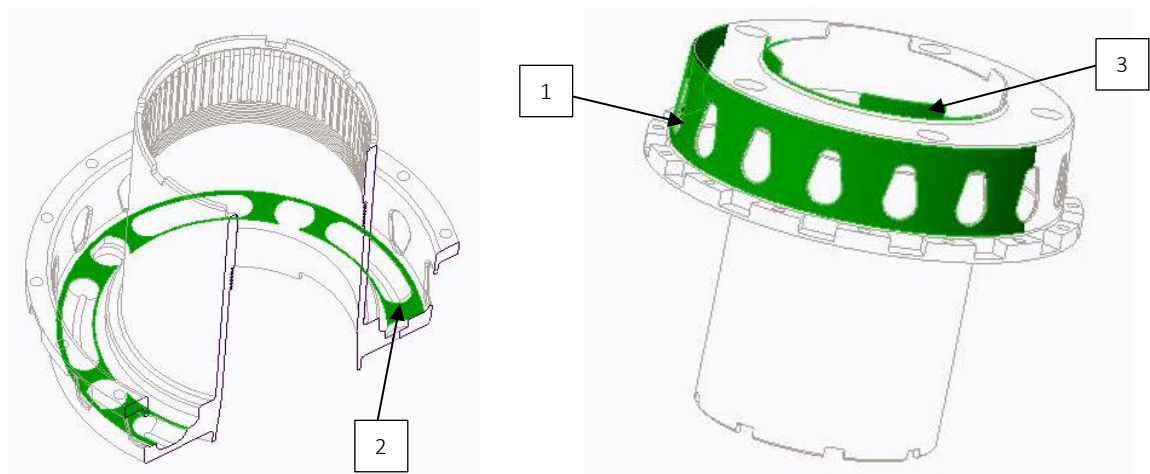


Figure 4.33. Areas that have been optimized in the Hub

4.12.1.3 Thermal Analysis of Hub and Cup

To investigate the impact of the heat load with Boundary Conditions in Figure 4.32. The Cup is not included in this figure, and the heat load is applied evenly distributed through the entire assembly of Cup and Hub as a simplification. For the magnitude of the heat load see Table 4.6. The new designed Cup need to be manufactured in either Steel C55 or the 15CDV6 and is analysed in Figure 4.34 due to equal thermal coefficients of $11.8 \cdot 10^{-6} / ^\circ\text{C}$. The Cup in Aluminium 7075-T6 is presented in Figure 4.35. The Hub is in Steel 300M for both analyses. The aluminium can make an advantage in the lower density and was therefore interesting. The result of this analysis shows that the Cup manufactured in 15CDV6 with equal thermal coefficient as 300M, see Table 4.2 is preferred and selected for the Cup due to the von Mises stresses in Figure 4.34. The stresses are below the yield strength of 790 MPa, see Table 4.2 and the Margin of Safety this gives in Table 4.7. In Figure 4.35 the Aluminium 7075-T6 with a tensile strength of 572 MPa, see Table 4.2 will begin plastic deformation due to heat load. The stress concentrations in the analyses are neglected due to the Boundary Conditions.

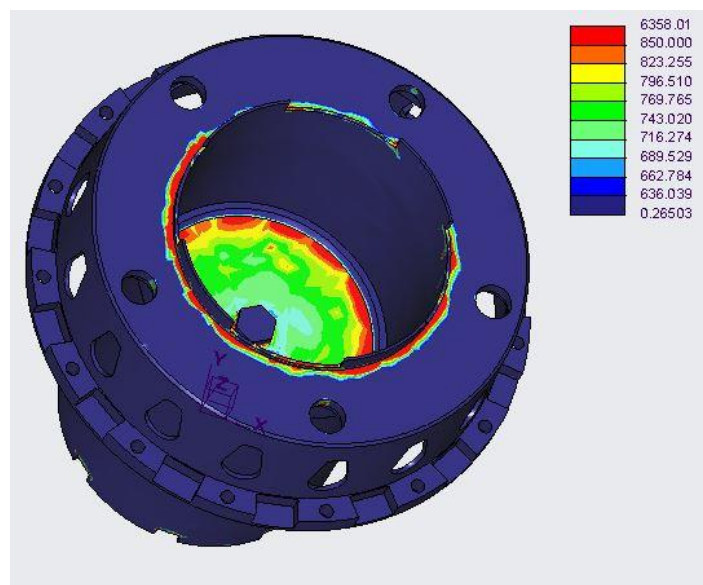


Figure 4.34. von Mises stresses - Cup in Steel C55 or 15CDV6 [MPa]

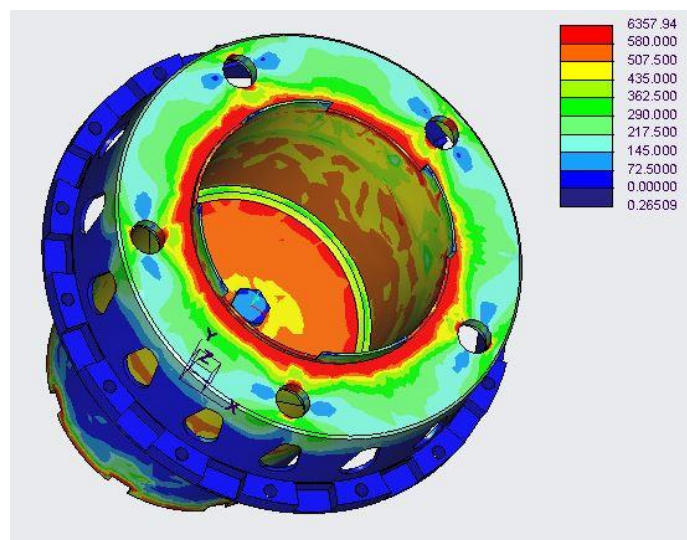


Figure 4.35. von Mises stresses - Cup in Aluminium 7075-T6 [MPa]

4.12.1.4 von Mises stress Analysis of the Hub with forces and moment applied

The von Mises stresses in the Hub is approximate 1150 MPa, with singularities in sharp edges neglected. See Figure 4.36 that presents areas of stresses in the full Hub. Figure 4.37 presents a closer view of the areas with large stresses. Figure 4.38 presents the Hub in deformed with 20% scale.

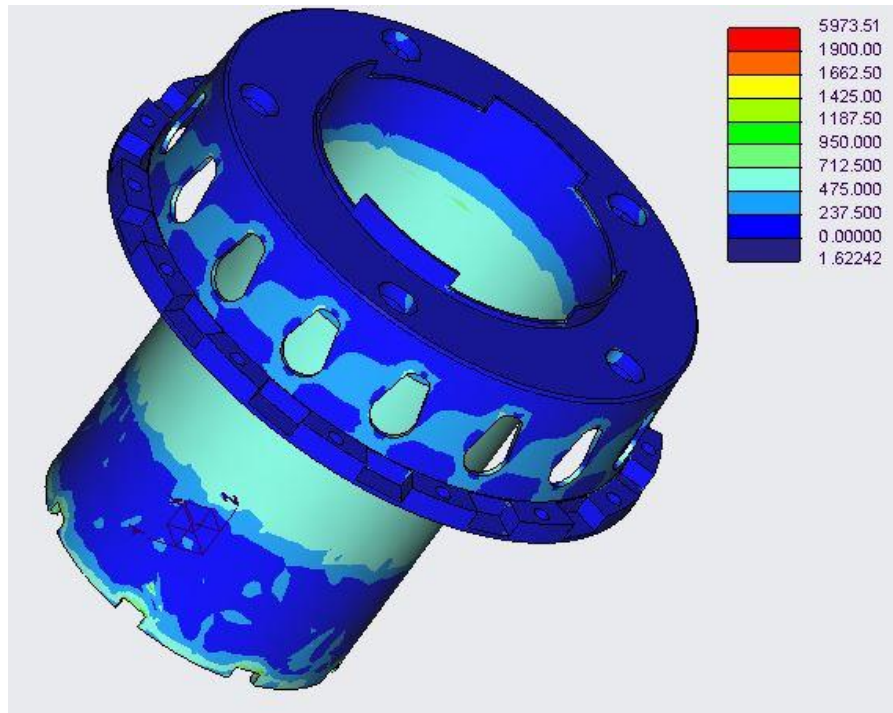


Figure 4.36. von Mises stresses [MPa]

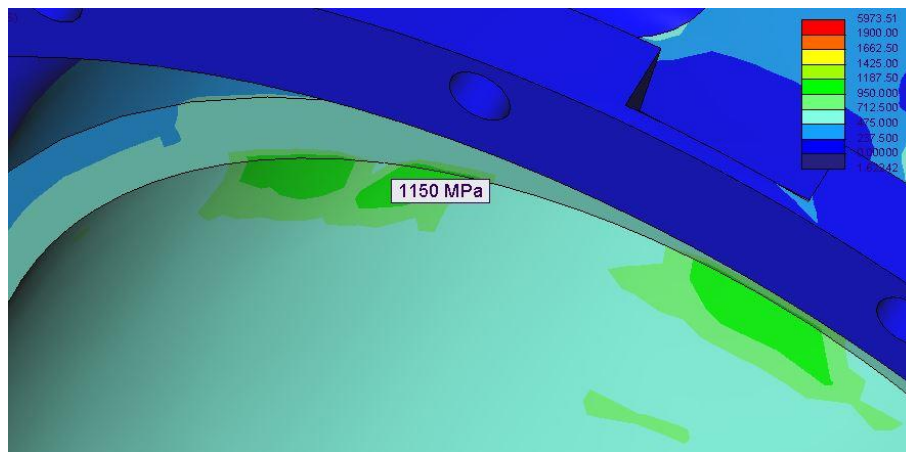


Figure 4.37. von Mises stresses detailed view [MPa]

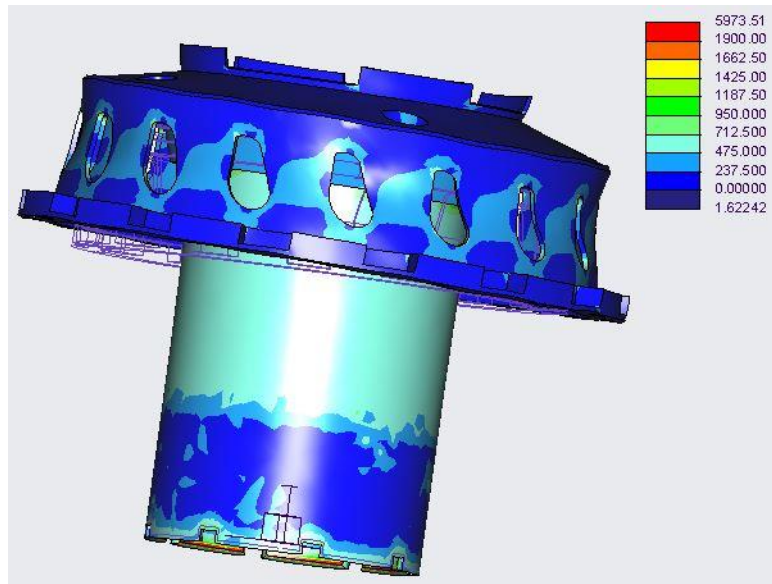


Figure 4.38. von Mises stresses deformed 20% scaled [MPa]

4.12.1.5 Strain Analysis of the Hub with forces and moments applied

The strain analysis of the Hub is presented in Figure 4.39. The strain reaches approximate 0.00518. The strain analysis is not used to optimize the Hub, and only used to analyse the tension in the material.

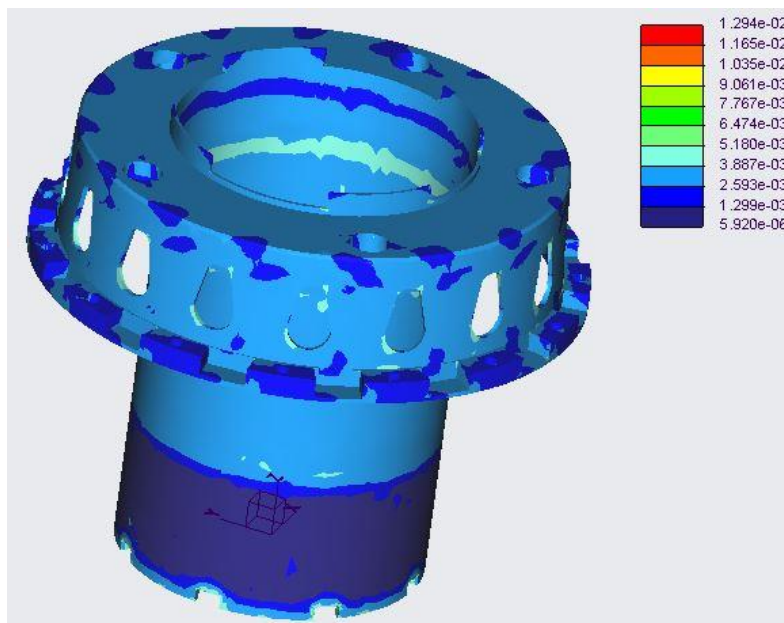


Figure 4.39. Max Principal Strain in the Hub

4.12.1.6 Displacement Analysis of the Hub with forces and moment applied

A displacement analysis is performed, and result presented in Figure 4.40 shows an undeformed Wheel Hub. The displacement presented is the magnitude of displacement in x , y , z -directions. The displacement of maximum approximate 0.489 mm is acceptable and will not affect the Hub, Ring or upright negatively. Figure 4.41 presents the Hub in deformed with 20% scale.

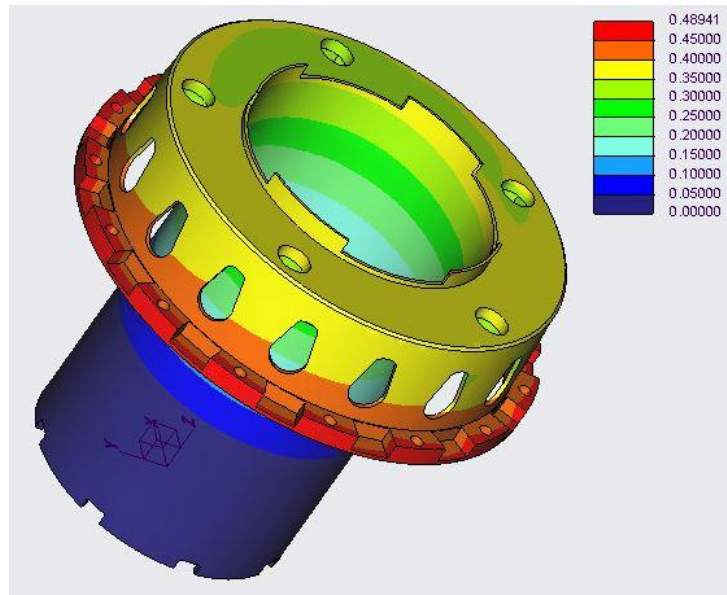


Figure 4.40. Displacement Magnitude [mm]

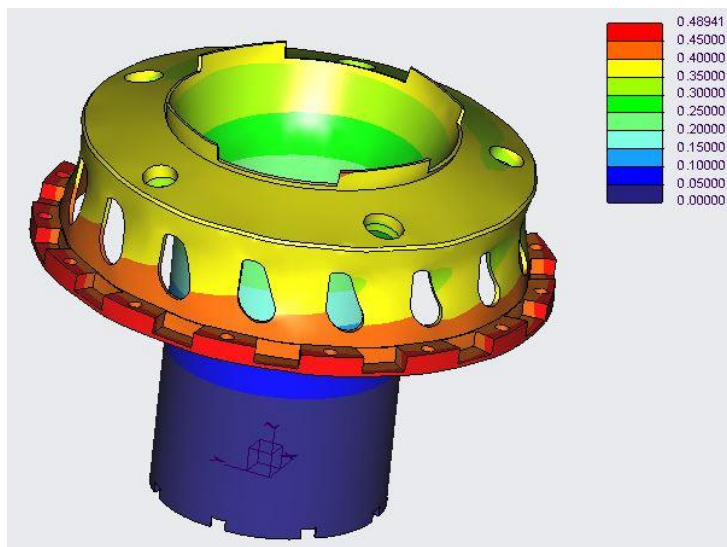


Figure 4.41. Displacement Magnitude deformed 20% scaled [mm]

4.12.1.7 Failure Index of the Hub

A function used in Creo, Failure Index is applied to detect failure of the material in the Hub. A Failure Index above 1, meaning a failure of the material. Figure 4.42 presents the result of the analysis and shows that the Hub reaches an index of approximate 0.5. This is also calculated and discussed with the Margin of Safety in Section 4.12.1.9.

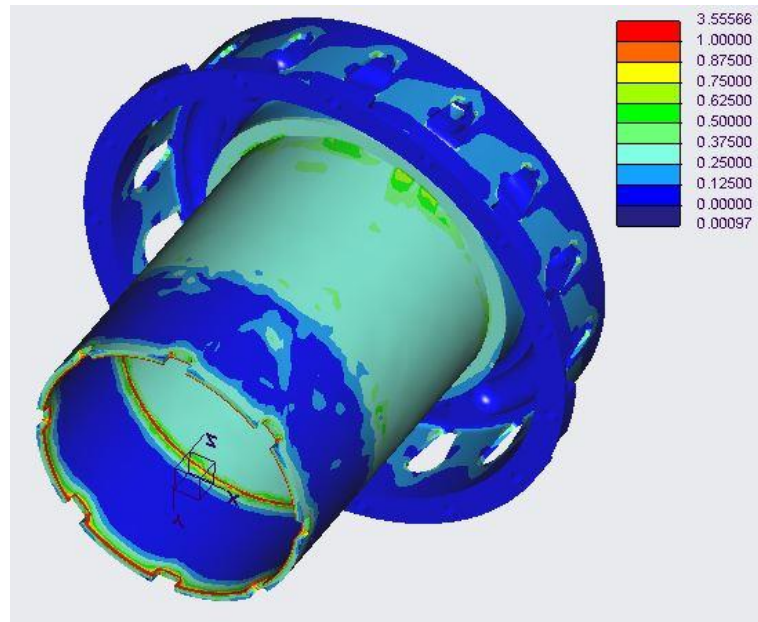


Figure 4.42. Failure Index - Hub

4.12.1.8 Finite Element Analysis Full Assembled Model

To prove all results from the parts analysis, a full assembled analysis is performed to the model. This analysis is computational heavy and consumes a lot of time but seem important to perform at the end of the development process. Final test the Wheel Hub is analysed with, set as a reference if the design fulfils the requirements and tests all parts assembled. In this analysis the heated load and the braking torque is applied on the Brake Disk, see Figure 4.43 number 1. Other Boundary Conditions used as previous, see Figure 4.32 and contact simulation between the Brake Disk and the Hub at all interfaces pointing in rotation about centre axle of the Hub, number 2. The Ring is constrained only on the Hub together with the Screws (no initial contact between the Ring and Brake Disk). This are performed to make the simulations realistic as possible and evaluate the simulation part by part. The material in the Ring, Brake Disk and Screws are unknow in the extend to that it is steel, the parts are not analyses due to stresses and a general thermal coefficient of steel ($11.8 \cdot 10^{-6} / ^\circ\text{C}$) (AZoM, 2018) are assumed for these parts. The Hub and Cup are analysed in the specified materials 300M in the Hub and 15CDV6 for the Cup. In Figure 4.44, Figure 4.45 and Figure 4.46 shows the von Mises stresses deformed 20% and the assembled Wheel Hub will pass the analysis and is expected due to work.

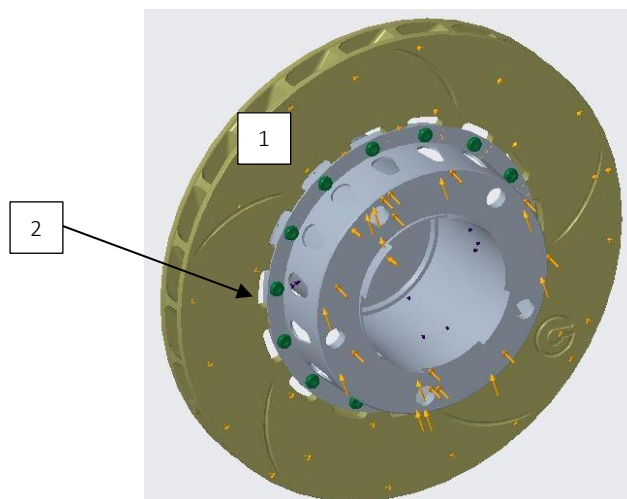


Figure 4.43. Assembled Wheel Hub Boundary Conditions

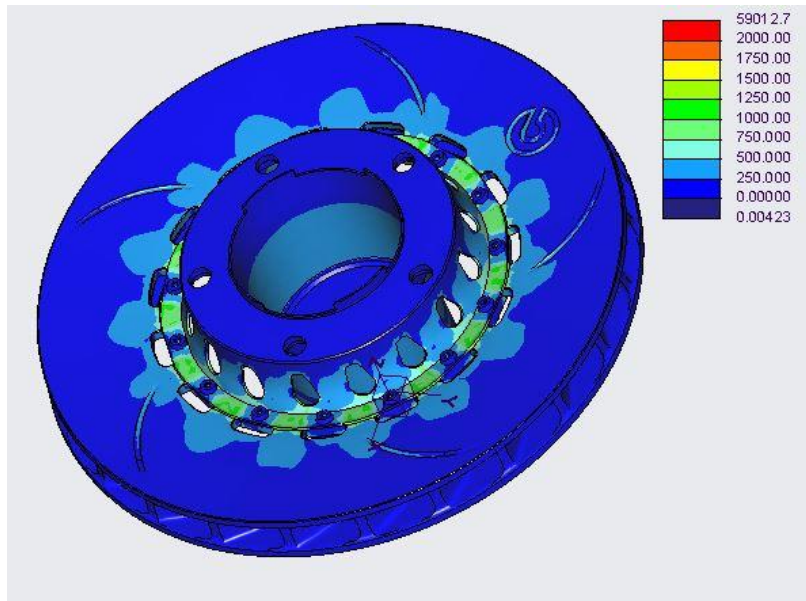


Figure 4.44. Assembled Wheel Hub von Mises stresses deformed 20% scaled [MPa]

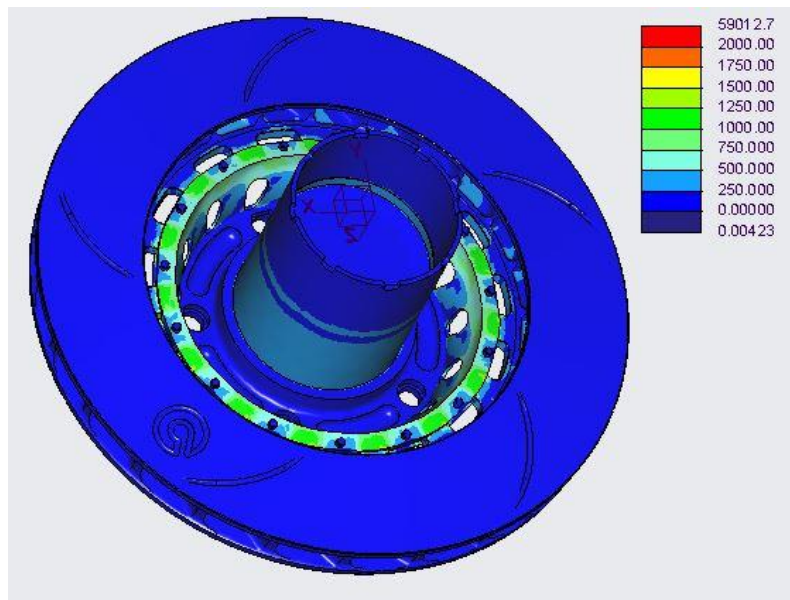


Figure 4.45. Assembled Wheel Hub von Mises stresses deformed 20% scaled [MPa]

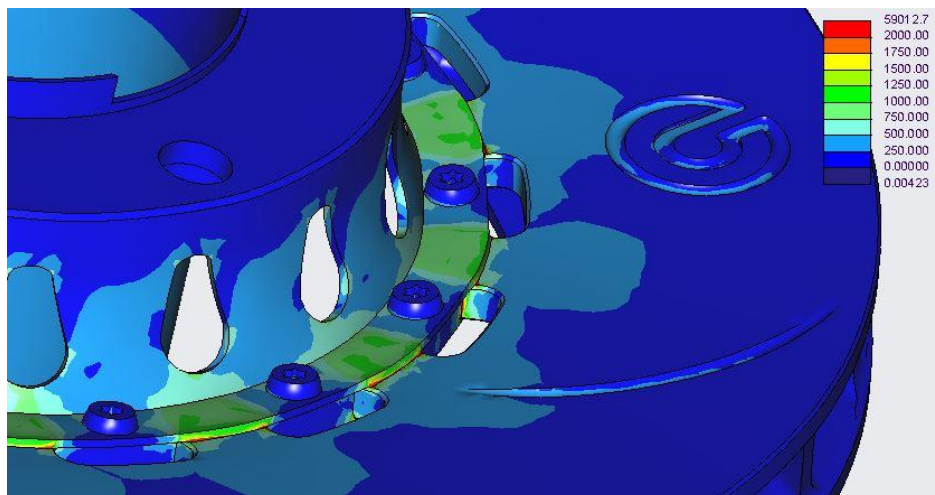


Figure 4.46. Assembled Wheel Hub von Mises stresses deformed 20% scaled detailed view [MPa]

4.12.1.9 Margin of Safety

The Finite Element simulation-results and the design analysis are evaluated carefully due to the Safety Factor is used on the forces applied. To show the Margin of Safety of the Hub, Equation (4.28) are used (Collins, Busby, & Staab, 2010).

$$\text{Margin of Safety} = \left(\frac{\text{Yielded strength}}{\text{Measured stress}} \right) - 1 \quad (4.28)$$

The Margin of Safety calculated for the Finite Element-results on the Hub, which is considered most critical loaded are presented in Table 4.7.

Table 4.7. Margin of Safety

Hub	Yield strength (of used material) [MPa]	Measured von Mises stresses [Mpa]	Margin of Safety
Figure 4.36	790	507	0.56
Figure 4.38	1980	1150	0.72
Figure 4.48	1980	1250	0.58

5 Results and Discussion of the Re-designed Wheel Hub

The result of the theoretical background, work in CAD and Finite Element Analysis. Each part in the Hub is described, and the total assembly shown in Figure 5.2 and a comparison of the current and the re-design are presented in Figure 5.1 with a section-view. The re-designed Hub with the Brake Disk Adapter integrated gives a compact design and reduces the number of parts.

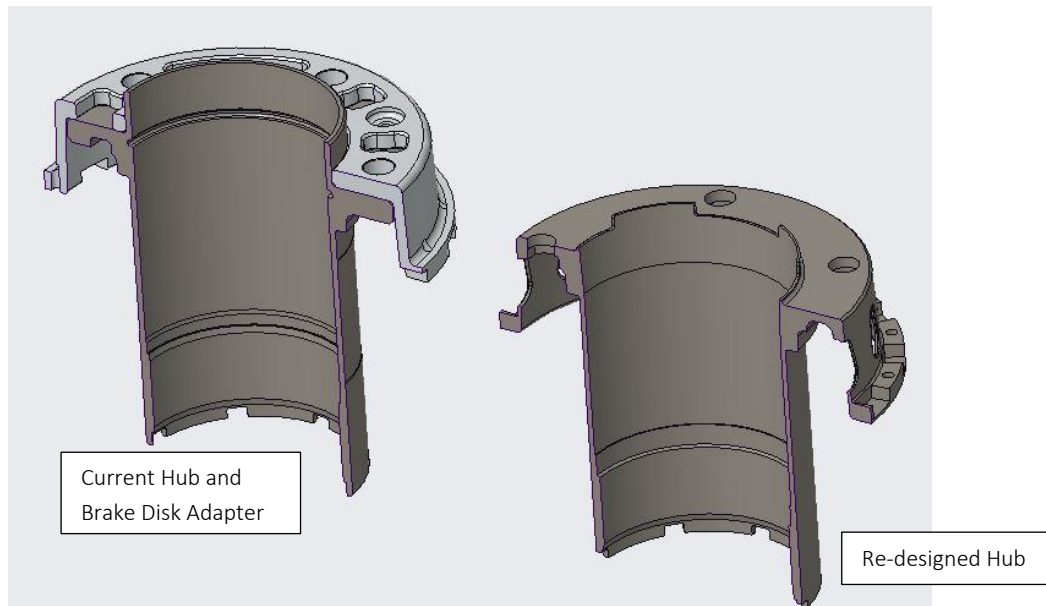


Figure 5.1. Result of Current and Re-designed Hub's

Figure 5.2 presents a rendered assembly of the re-designed Wheel Hub fitted in the current upright (partly visible in the figure) and CV-joint (only inner joint and driveshaft visible in the figure). This is performed both to demonstrate the design and that the Hub will be able to replace the current Hub with retained function. Each part and function are described in Section 5.1 to 5.6.

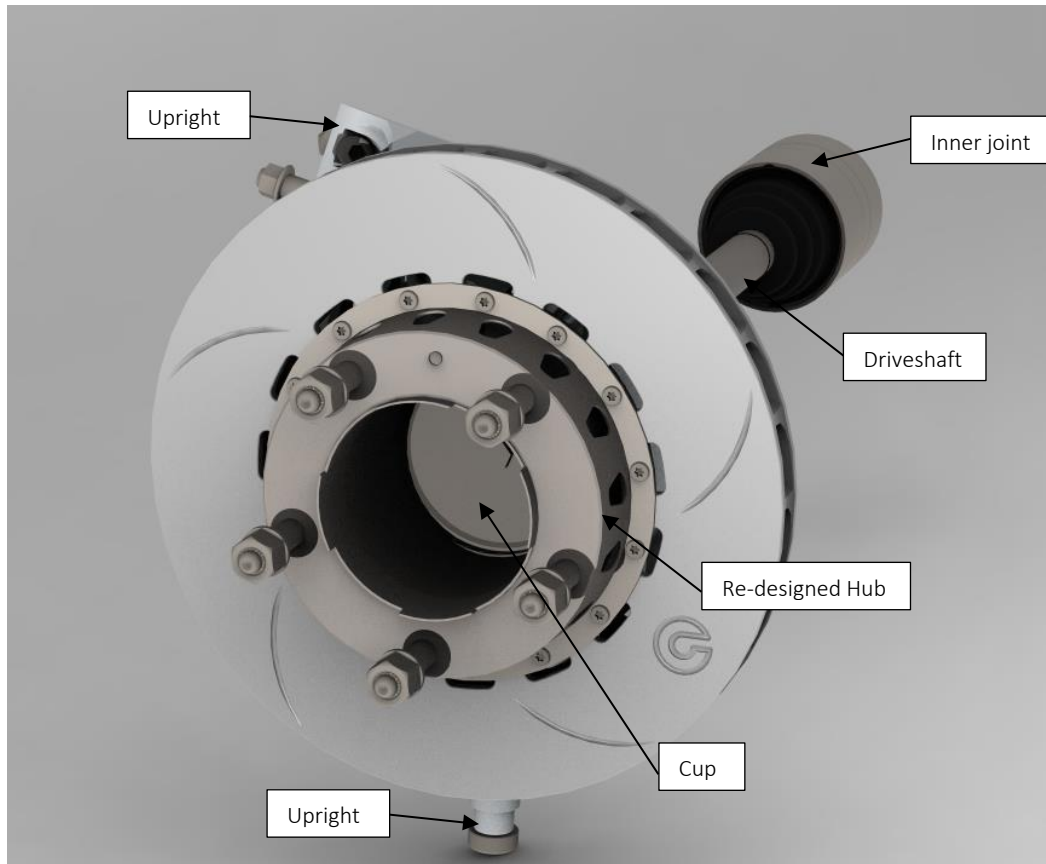


Figure 5.2. Re-designed Wheel Hub - Assembly

The current design optimized is presented in Section 4.11.2 and the re-engineered design with best advantages of mass and performance are discussed in 5.1 to 5.6. Section 5.7 performs a comparison between the current design, optimized and the re-designed in Table 5.1. The aims for this project described in the Pre-study, Section 2.1.1 is evaluated at the end of the project to make sure all goals are satisfied. A list of all objectives and the outcomes have been used to find the re-designed Wheel Hub presented from this project;

- **Estimation of acting loads**

The loads acting on the Wheel Hub were calculated through a Data Analysis to get accelerations in x , y , z -directions. This information was used in both dynamic and static analyses to estimate the loads. The uncertainty and special case-forces covered by a Safety Factor. The result of this work is presented directly in Section 4.9.

- **Comparative Design Analysis**

By comparing two Wheel Hub's, the current and a Hub from Pankl Systems the advantages and disadvantages were collected. The knowledge and result of this analysis are performed in Table 4.1 and used through the project, and the re-designed Wheel Hub fulfills the interesting advantages.

- **Optimization**

After the Pre-study and Concept Screening, a CAD-model was performed. Parameters of the Hub were set as variables and simulations were performed to find the optimal geometry of the Hub with respect to mass vs. the strength which gives an optimal design.

- **New design**

Presented in Figure 5.1 and 5.2 the mass-reduced Wheel Hub was performed. The model was handed over to EKS as STEP-file and EKS has all rights to perform changes, evaluate the result and decide if the Hub fulfills the requirement.

5.1 New designed Wheel Hub - With Brake Disk Adapter integrated

The design with the Brake Disk Adapter integrated in the Hub gives the opportunity to select a new material of the Hub due to the need of manufacture a complete new part. The design with an Adapter for the Brake Disk integrated in the Hub makes it possible to reduce material and minimizes the number of parts. To re-design the Hub and changing material makes it possible to adjust the inner diameter of the Hub and make another solution for the axial fixation of the CV-joint (previously the function of the Socket). The inner diameter of the Hub is now 1.5 mm larger, 120 mm from the attachment surface for the rim, see number 1 in Figure 5.3. A rendered assembly of the complete Wheel Hub in Figure 4.31. The outer diameter of the Hub is identical as the current, and no changes are made to the interfaces for the Wheel Bearing or its position, see Figure 5.5. This, due to the possibilities to use the Hub in the existing upright on the car.

A section of the re-designed Hub is presented in Figure 5.3 to show the Hub. The threads, number 2 and splines, number 3 for the Cup and CV-joint (splines equal as current Hub).

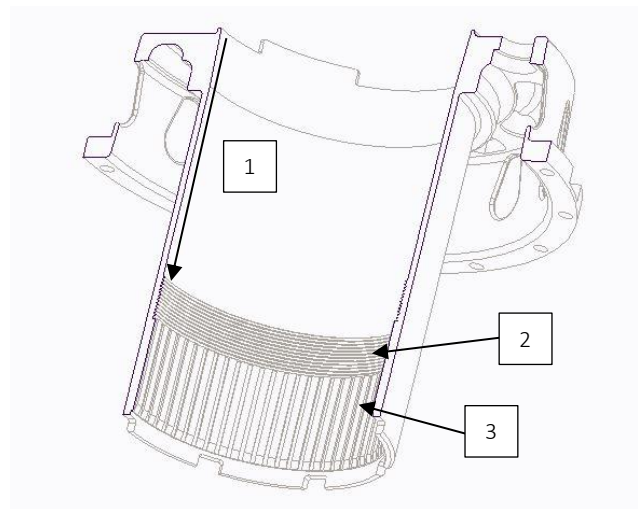


Figure 5.3. Skeleton section of the Hub

5.2 Threads discussed for the CV-joint and Cup

Instead of the current Socket and the Retaining ring a Cup (see 5.5) is performed to fix the CV-joint axial in place. To make this solution intact with a tighten Cup, the threads is designed, see Figure 5.5 with a Left-Hand thread on the Left-side-Hub and Right-Hand on the Right-side-Hub. This will result in that two versions of the Hub need to be manufactured, one special for each side. The advantages of this is considered, and a decision to perform this solution is made to secure the CV-joint.

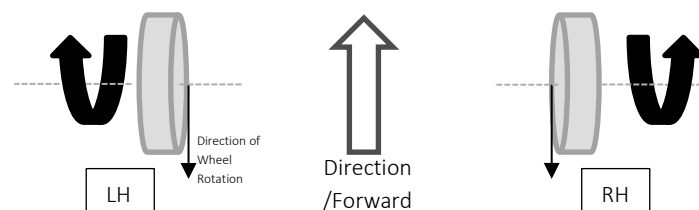


Figure 5.4. Right-Hand and Left-Hand threads defined

The area including splines to transfer torque from the CV-joint copied from the current Hub. For comparing the current design, see Figure 4.31 in Section 4.11.

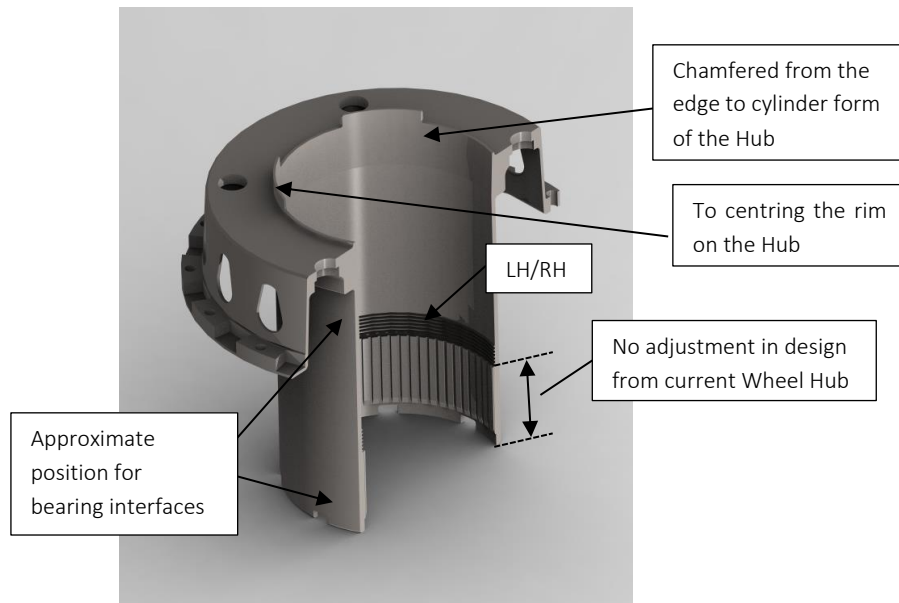


Figure 5.5. Wheel Hub - New design

5.3 Centring ring for the rim

The centring ring on the Hub is analysed and the material is heavily reduced due to the low forces acting on the edge, either moments or radial/axial forces appear in normal use. This design is selected to be as mass optimal as possible, see the new and optimized centring ring in Figure 5.5.

5.4 Interfaces for Brake Disk

The interfaces for the Brake Disk on the current Brake Disk Adapter is designed to assemble the Brake Disk when, not assembled on the Hub/car. Due to this, a new solution is performed when the Brake Disk Adapter is integrated in the Hub and cannot be removed to fix the Brake Disk. The selection of Brake Disk is made by EKS (Ljungberg, 2018) and the solution need to fit the interfaces of the Disk and be able to assemble with Wheel Hub in the upright (on the car). For drawing of the Brake Disk from Brembo®, see appendix.

The new solution of the interfaces and fixation for the Brake Disk is presented in Figure 5.6 and Figure 5.7. The Brake Disk is fixed in position with the current solution of a Ring. This Ring prevents the Brake Disk to move in the axial direction. The projections in the intersection transfers the torque to the Hub generated during braking. The Brake Disk is “floating”, a floating disk avoiding thermal stress and cracking. The Disk can expand in a controlled symmetrical way and minimize the heat transfer to the Hub when the temperature riser caused by friction between Brake Disk and Brake Pads. The moment acting on the Hub only affects the interfaces with the rotation due to that the Disk are not fixed in the position. The Ring and Screws to fix the Brake Disk in axial direction is used as the current.



Figure 5.6. Wheel Hub and Brake Disk - Exploded view (Half-view)

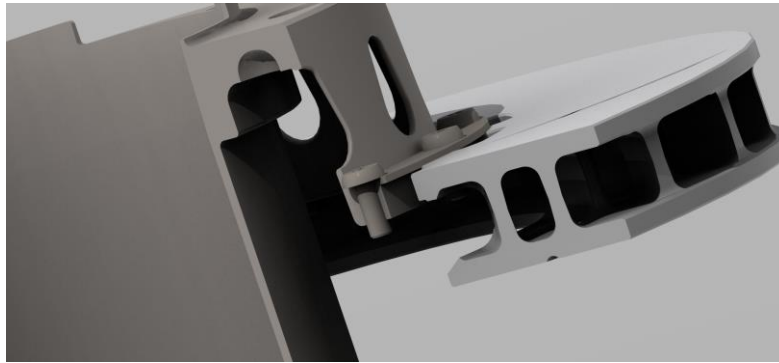


Figure 5.7. Wheel Hub and Brake Disk - Assembled (Half-view)

5.5 Cup

The Cup is a new designed and manufactured part. The Cup is manufactured in Steel 15CDV6 due to minimize the effect of thermal expansion explained in Section 4.12.1.3. A M13 hexagonal nut is placed in the centre of the Cup to make it easy to assemble and disassemble the Cup in the Hub. The edge of the Cup is made with a 1.25 mm pitched thread, see Figure 5.8.

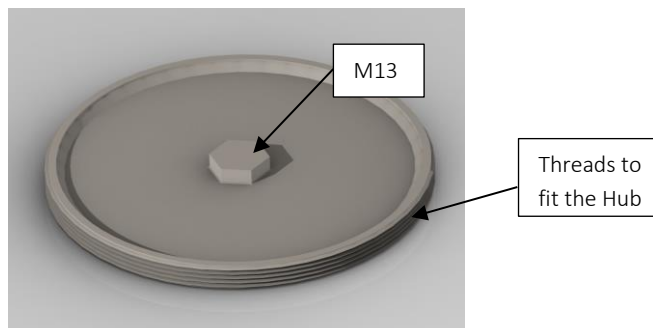


Figure 5.8. Cup

Figure 5.9 shows a Quarter section-view of the Hub with the Cup assembled in place. The red-dotted line represents the top-edge of the CV-joint when everything is assembled correctly. The CV-joint is not included to show the new manufactured and re-designed parts properly.

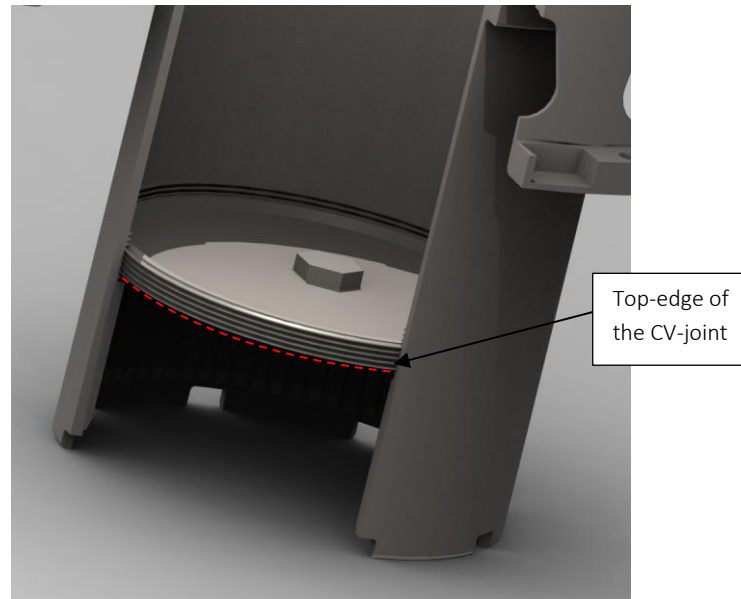


Figure 5.9. Cup assembled in the Wheel Hub (Quarter section-view of Hub)

5.6 Tap

The Tap performed is made in the same material as the current, Aluminium 7075-T6. The current part can be modified by lathing because of only geometrical material is removed, but a new part is recommended. The O-ring seal to protect the CV-joint from dust and damp are the same used in the current due to no re-designed geometry in that region, see Figure 5.10. The centred M8x1.25 hole is used to disassemble the Tap. See Figure 5.11 for an assembly of the Tap placed with the locking ring in the CV-joint as in the current design.

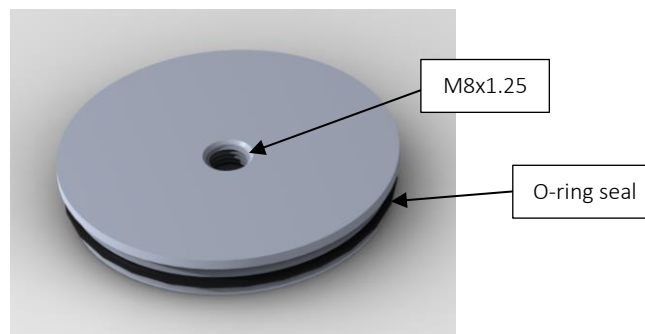


Figure 5.10. Re-designed Tap

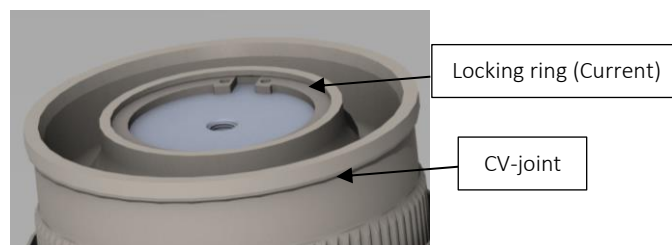


Figure 5.11. CV-joint with re-designed Tap

5.7 Masses of the current design, the Optimized and Re-designed Wheel Hub's

The objectives in this project is to reduce the mass of the total Wheel Hub. A summation of all containing parts with specific masses, see Table 5.1. In the developed design of the current Hub with

optimization a new Socket is performed in Aluminium 7075-T6 that reduces the mass of the Socket with retained function. Figure 5.12 presents a comparing between the two designs.

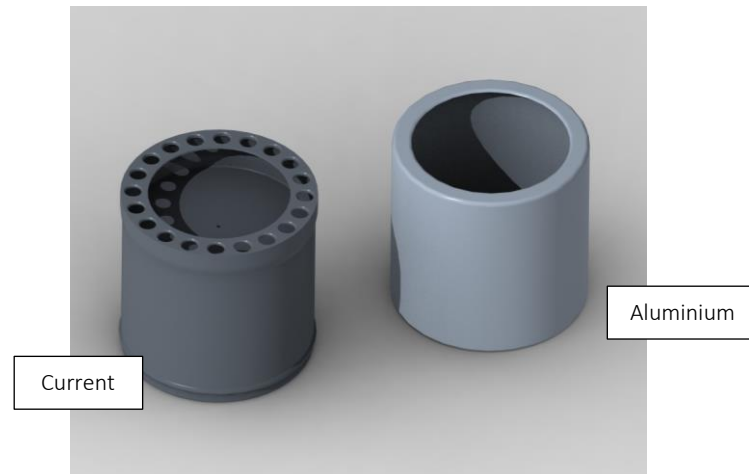


Figure 5.12. Current and Aluminium Sockets

Table 5.1 contains both physical measured masses of the current parts, and expected masses calculated in Creo with the material properties. Seen in the Table, a reduction in mass for the optimized Hub and Socket in aluminium are 15% and the re-designed complete Wheel Hub is 25%, or 843 grams per wheel.

Table 5.1. Specific masses - Current, Optimized and Re-designed Wheel Hub's

Specific mass of parts	Current design today		Current design developed design with optimization	Developed design with integrated Brake Disk Adapter
	Experimental (Physical mass measured by scale) [g]	Simulated mass (Measured in Creo) [g]	Simulated mass (Measured in Creo) [g]	Simulated mass (Measured in Creo) [g]
Hub	2102	2172	2030	2226
Socket	394	349	155	Not included
Tap	98	112	42	42
Locking Ring	18	18	18	Not included
Cup	Not included	Not included	Not included	195
Brake Disk Adapter	694	561	561	Included in the "Wheel Hub"
Total:	3306	3212	2805	2463
Change in Total per wheel:	-	-	501	843
Change per Wheel/Total on car:	-	-	-15%	-25%
Change in Total on car:	-	-	-2004	-3372
Total on car:	13224	12846	11220	9852

Note: Brake Disk and mounting ring/bolts on the brake disk adapter is included in the measurements

5.8 Simulation of the results in MATLAB® and Simulink®

To evaluate the result and advantages of the project, the MATLAB® and Simulink® model used to prove the theory, with an unsprung mass of 35 kg "base-line" (blue), the optimized Hub (orange) and the re-designed (green). The masses used for the optimized and re-designed Hub's is based on

simulations made in Creo, see Table 5.1. The data analysis and simulation are performed with a graph, see Figure 5.13. The graph is adjusted to the interval 0.55-0.64 seconds to present the region of interest. The three graphs with different variation of unsprung masses show clear that the re-designed Wheel Hub can follow the surface of the track better than the optimized due to both higher acceleration, velocity and displacement in the bump. Even if relatively small changes are presented, the overall advantage of the design in terms of reduced amplitude in the bump is interesting. This simulation presents only one bump, and on the track when the car travels with high speed and faces several bumps this will gain in even larger advantages.

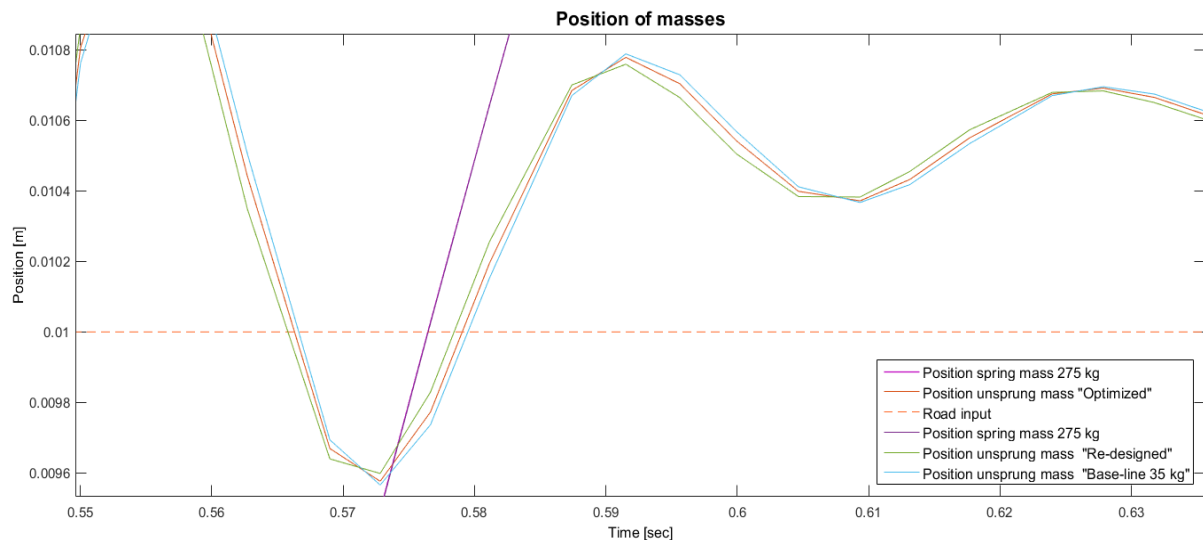


Figure 5.13. Simulation plot from Simulink of the different unsprung masses in Table 5.1 - Position

6 Discussion

6.1 Type of data collected from the car

The type of data collected and used in this project is restricted to the Section 4.9.3. To perform a relevant analysis to get the forces acting on the Wheel Hub the calculations in Section 4.9. These calculations are enough to find the forces, but information regarding the angles of the car would be good to have. The car was not equipped with a gyroscope at this time and this data (angles of roll, pitch and yaw) was calculated from the damper positions. To derive the angles from other data gives uncertainty and can result in a non-accurate value. It would be interesting to collect data from the car to compare with the calculated values, in both to prove the calculations and to find the accuracy.

6.2 Accuracy of the loads

One of the main impacts in this project are the non-accuracy of the estimated loads and forces acting on the Wheel Hub and containing parts. The assumptions are made with respect to both previous knowledge and to the extent that has been data or in-depth information available. The amount of data has been limited and no physical testing is possible to perform. The data and measurements used to calculate the loads is from a normal condition and therefore good information. In the calculations the friction coefficient is selected to $\mu=1$. This assumption may be too extreme and will never occur, a lower coefficient could represent a realistic case better. This is discussed and a decision to select the “worst case” was therefore selected.

6.3 Material properties - uncertainty

The uncertainty in the material properties is one of the most difficult part. No material data tested, and the properties used in this project is based on data given from manufacturers of the materials on their web-sites. This can clearly be recognised in Table 5.1 where the masses differ from the experimental tests performed. The differences may not only vary because of the material but may also depending on the CAD-models from EKS. The conclusions and decisions made in this project are taken by these analyses and may differ with other material data. The experimental masses and the simulated masses in Creo differ approximate 3% of the current Wheel Hub. This uncertainty is considered as small they can be neglected, and a credible result.

6.4 Selection of material

In the decision of material when a new Hub is designed, EKS had a recommendation to select the Steel 300M due to previous experience and the knowledge that this material is used in several other similar types of products. Therefore, and in the limited time of this project no further studies of other material and the fact of some disadvantages with the 300M. The material fulfils the requirements and withstands the loads and therefore selected to use in the Hub. The material has equal thermal coefficient as the current used steel. Due to this no further analysis of the interfaces between the Wheel Bearing or other parts and the Hub are performed. Other materials see Table 4.2 are all used in the Wheel Hub today and is therefore not analysed further in terms of hardness, thermal coefficient etc.

6.5 Long Time/fatigue - neglected

The material data, and information provided in the project does not include fatigue data. Due to this, only the static analysis is performed, and the fatigue is not considered. This can cause a problem while start using the Wheel Hub. Not in a short term but in the long term use the Hub can break during fatigue of the material. This is partially covered by the Margin of Safety in Section 4.12.1.9.

6.6 CAD-models

The CAD-models and 2D-drawings from EKS where given as STEP-files and PDF's. EKS uses different CAE-software than provided by University of Skövde. This forces the project to perform new models in Creo (used in this project) to perform changes and dimensions. The dimensions are picked from both the STEP-files by the measuring tool in Creo and the dimensions on the 2D-drawing. All models are compared with the STEP-files carefully to confirm the two models are identical. The uncertainty of this method could be if, and it is small problems with the STEP-files. The models do not include the splines, threads etc. which has to be neglected. Due to these problem, the CAD-model of the re-designed Wheel Hub need to be controlled carefully before manufacturing.

6.7 Re-designed Hub and Cup

When re-design is performed in the project, the focus is to re-design the including parts. The Socket is desired to minimize in terms of mass and therefore the Cup is performed. This design has the advantage in reduced mass compared to the current with the retained functionality. At the end of the project, an idea arises that this part could be excluded if the Hub is manufactured/designed with a shoulder that prevents the CV-joint to move outward in axial direction. The Cup and threads in the Hub can cause problems during long time use, if dust or dirt damages the threads. The Wheel Hub from Pankl System has the solution that driveshaft and CV-joint cannot be removed when the Wheel Hub assembled on the car. In a race with a limited time to change part this can cause problems,

therefore are, with some disadvantages the design with Cup selected. An easy and quick change of driveshaft and CV-joint can, in case of a broken part be very important to change easily!

7 Conclusions and Recommendations

The conclusions made while working through this project is that the possibilities to improve the Wheel Hub is large. The design developed in this project is a big step forward to reduce the unsprung mass of the car. The design will not affect the geometry of the suspension and therefore the behaviour of the car in that aspect. The advantages of change to the re-designed Hub will increase the acceleration of the car and improve the traction between tire and road. The limitations set in this project makes it difficult to make the changes needed to find the optimal design. Even if the design will improve the car by making small changes can an advantage in changing the upright and suspension geometry an even more innovative design with less unsprung mass and advantages in suspension geometry, heat flux etc.

The design (optimized current Wheel Hub) presented in Figure 5.12 reduces the mass with 15% and can be performed with small changes and new parts. This design is not fully optimized but will reduce the total mass of the Wheel Hub which was the objectives. Recommendations to EKS is to evaluate the re-designed Hub and compare the result of this project to find their best decision the best way to improve the unsprung mass of the car.

8 Future Work

- To collect even more data from the car to evaluate the accuracy of the loads calculated and acting on the Wheel Hub. Not only the vehicle dynamic-parameters used in this project but also, by using strain gauges on the Hub to measure strains in the Hub while use. And by temperature sensors to measure the heat load.
- Evaluate material properties used in this project with manufacturers of the material and perform research of any other materials is possible to use.
- Re-fine the simulations and Boundary Conditions to perform even more realistic simulations.
- Produce a prototype of each part to evaluate the Wheel Hub in a 1:1 scale and test on the car.

References

- Aircraft Materials Ltd. (2018, 02 19). Retrieved from <https://www.aircraftmaterials.com>
- Anderson, M., & Harty, D. (2010). Unsprung Mass with In-Wheel Motors - Myths and Realities. *AVEC* (pp. 261-266). Loughborough: Loughborough University.
- AZoM. (2018, 05 04). Retrieved from <http://www.azom.com>
- Collins, J. A., Busby, H., & Staab, G. (2010). *Mechanical Design of Machine Elements and Machines*. Hoboken, USA: Wiley.
- Dhakar, A., & Ranjan, R. (2016). Force calculation in upright of a FSAE race car. *International Journal of Mechanical Engineering and Technology*, 7, 168-176.
- Dynamic Materials Ltd. (2018, 02 19). Retrieved from <https://www.dynamicmetalsltd.co.uk>
- EKS RX. (2018, 04 18). Retrieved from <http://www.eksrx.com>
- Engineeringtoolbox. (2018, 05 23). Retrieved from <https://www.engineeringtoolbox.com>
- Galal, A. H. (2015). Car Dynamics using Quarter Model and Passive Suspension, Part II: A Novel Simple Harmonic Hump. *IOSR Journal of Mechanical and Civil Engineering*, 12, 93-100.
- Genta, G. (1997). *Series on Advances in Mathematics for Applied Science - Vol. 43: MOTOR VEHICLE DYNAMICS - Modelling and Simulation* (4 ed.). Toh Tuck Link, Singapore: World Science Publishing Co. Pte. Ltd.
- Jansson, P., & Grahn, R. (2013). *Mekanik*. Lund: Studentlitteratur.
- Jiang, K., Pavelescu, A., Correa Victorino, A., & Ali, C. (2014). Estimation of vehicle's vertical and lateral tire forces considering road angle and road irregularity. *17th International IEEE Conference on Intelligent Transport Systems* (pp. 342-347). Qingdao, China: 17th International IEEE Conference on Intelligent Transport Systems.
- KAZ Technologies. (2018, 02 20). Retrieved from <http://www.kaztechnologies.com>
- Ljungberg, J. (2018, 02 15). Technical Director, EKS RX. (E. Andersson, Interviewer)
- Messner, P. B., & Tilbury, P. D. (2018, 02 19). Retrieved from Control Tutorials for MATLAB and Simulink (CTMS): <http://ctms.engin.umich.edu/CTMS/index.php?example=Suspension§ion=SimulinkModeling#2>
- Milliken, W. F., & Milliken, D. L. (1997). *Race Car Vehicle Dynamics*. Warrendale, USA: SAE International, Inc.
- MindTools. (2018, 05 03). Retrieved from https://www.mindtools.com/pages/article/newTMC_07.htm
- NASA. (2018, 05 03). Retrieved from <https://www.grc.nasa.gov/www/k-12/airplane/newton2.html>
- ProjectManagementSkills. (2018, 05 03). Retrieved from <https://www.project-management-skills.com/project-risk-management.html>
- SAE International. (2018, 02 23). Retrieved from <https://www.sae.org>
- Sajjan, B., Parthasarathy, A., Kiran P, S., & Kumar K N, V. (2016, 8). Product Design and Development of Wheel Hub for an All-Terrain Vehicle (ATV). *International Journal of Engineering Research & Technology*, 5, 504-509.

- Segers, J. (2014). *Analysis techniques for racecar data acquisition - Second Edition*. Warrendale, USA: SAE International, Inc.
- Sharma, P., Saluja, N., Saini, D., & Saini, P. (2013, 7). Analysis of Automotive Passive Suspension System with Matlab Program Generation. *International Journals of Advancements in Technology*, 4, 115-119.
- Sharma, R., & Nain, R. (2015, 10). Design and Weight optimization of wheel assembly components using FEA for BAJA. *International Journal of Aerospace and Mechanical Engineering*, 2, 14-17.
- Sundström, B. (1998 (edit. 2013)). *Handbok och formelsamling i Hållfasthetslära* (8 ed.). Stockholm: Department of Solid Mechanics, Royal Institute of Technology.
- The International Institute for Sustainable Development (IISD). (2018, 05 04). Retrieved from <http://www.iisd.org/topic/sustainable-development>
- The Mathworks Inc. (2018, 02 19). Retrieved from Mathworks Documentation: <https://se.mathworks.com>
- Vitthal Wable, P., & Sanjong Shah, S. (2017, 8). Design Analysis & Optimization of Hub Used in FSAE cars. *International Journal of Innovative Research in Science, Engineering and Technology*, 6, 16799-16808.
- Wollstrand, M., & Sallbring, A. (2015). *Optimization Driven Design Process for Vehicle*. Lund: Lund University Publications (LUP).

Appendices

Work Breakdown and Time Plan - Before project start

A plan including deadlines from the University of Skövde, Ulf Stigh, are used to perform a Gantt-schedule for the project, see Figure A-1. The information known of the project at this point are set in the plan and can be adjusted during the project if needed. A general plan and two specific plans are made, Pre-study in Figure A-2 and development in Figure A-3 to make it more detailed. The dates in the planning and the work are supposed to be done at this time to follow the plan.

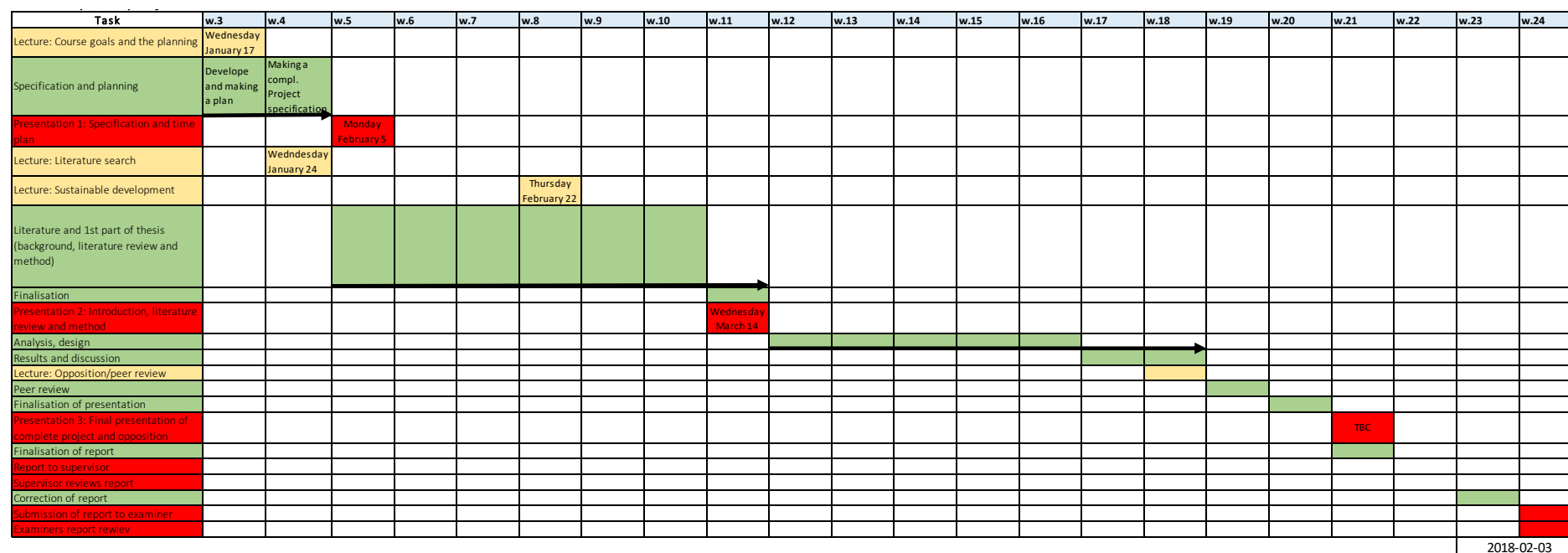


Figure A-1. Gantt Plan Full Project

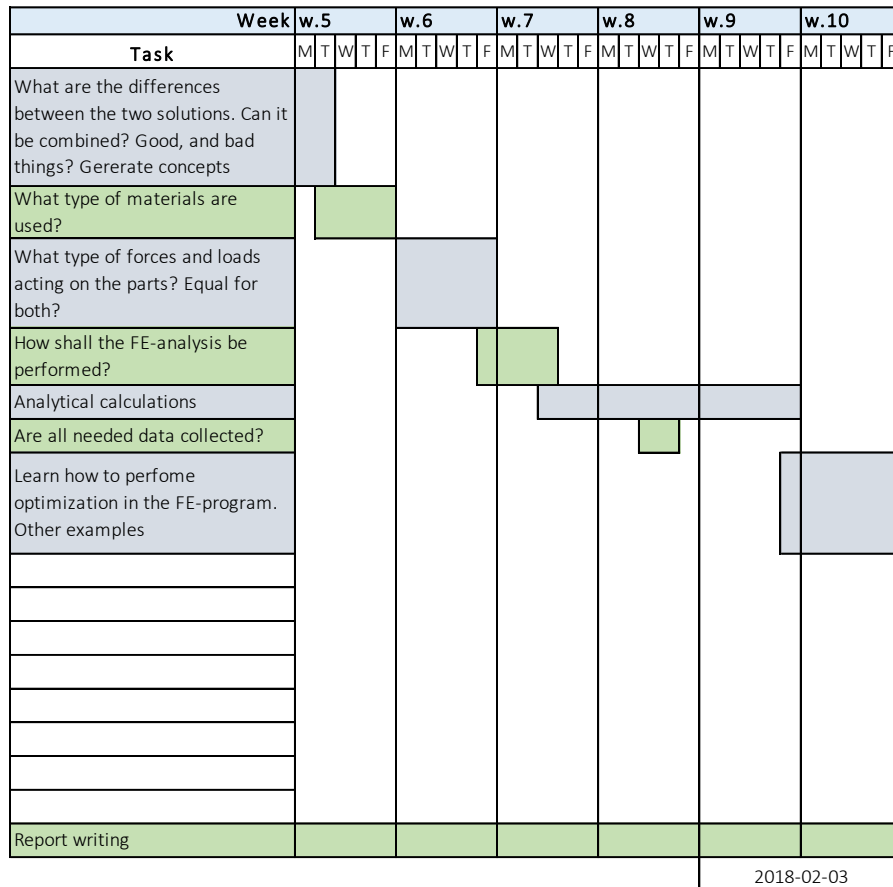


Figure A-2. Gantt Plan Pre-study

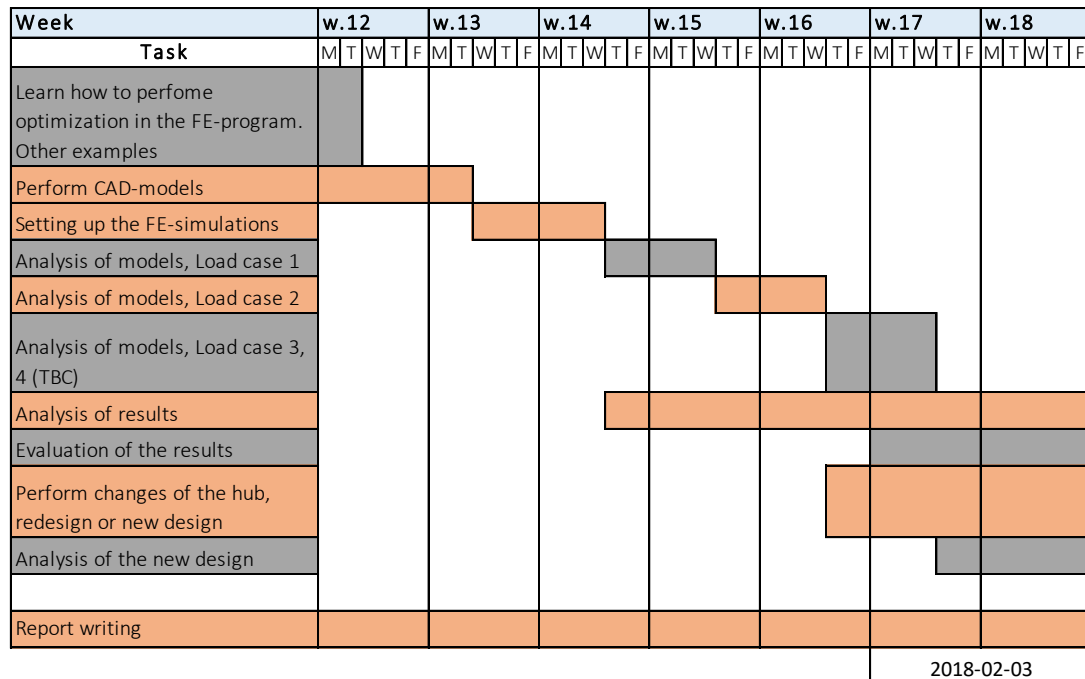


Figure A-3. Gantt Plan Development process

Work Breakdown and Time Plan - After project comments

Through the project, the plan is controlled and followed, no changes made, and the plans developed in the project start where followed in the entire project. The Gantt Plans performed before the project start become helpful through the whole project. The project proceeds as expected with only minor changes, see Figure A-4 and gives possibilities to step back and refine previous work when the project is ahead of the schedule.

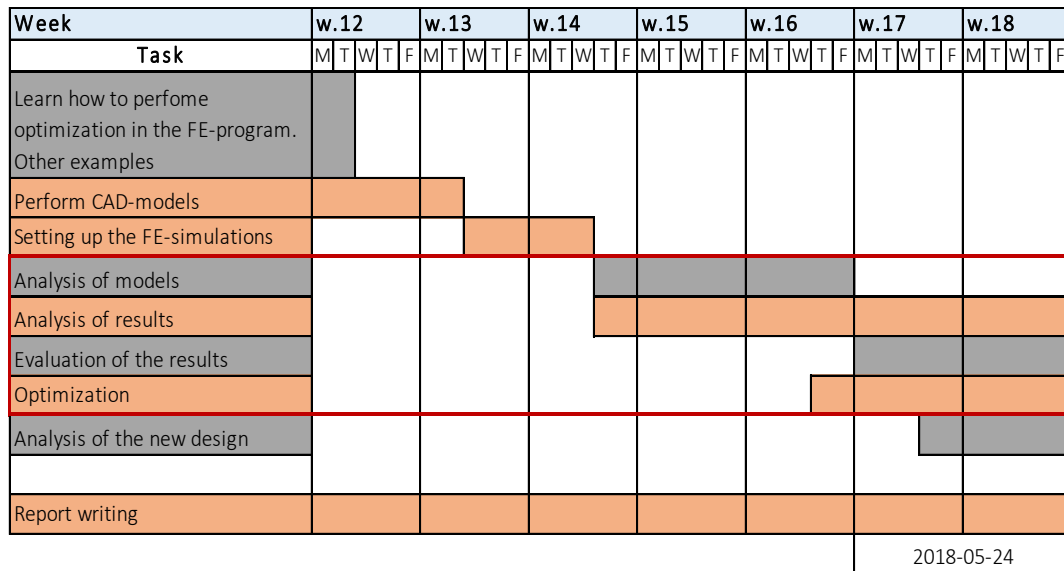


Figure A-4. Gantt Plan Development process - After project

Project Risk Analysis

A Project Risk Analysis is performed before the project starts and these tasks need to be carefully complete during the project (ProjectManagementSkills, 2018). For the analysis see Table A-1.

A Risk Analysis is used in projects to identify and manage risks that can appears thru the process and avoid them in the in the opportunity it is possible to do it (MindTools, 2018). As they mention on Project Management Skills a “*Project risks exist because of uncertainty. There is always the possibility that something known or unknown could impact the achievement of your project's goals. Risk management is about being prepared to handle these risks*” (ProjectManagementSkills, 2018).

Table A-1. Project Risk Analysis

		Likelihood		
		High	Medium	Low
Impact	High	Problems in CAD-program	Finding accurate material data	Unable to get right data
	Medium	Optimization limits in the FE-software	Unable to calculate right forces on the hub	Manufacturing problems
	Low	Wrong assumptions	Lack of time to perform all tests	Misscalculations

Project Risk Analysis - After project comments

The Project Risk Analysis where followed and controlled carefully through the project and the highlighted risks also becomes the biggest problems in the project. With help of the analysis performed before the project start, the problems appear in an early state and could handle them systematically to proceed with the project at time.

Drawing Current Hub

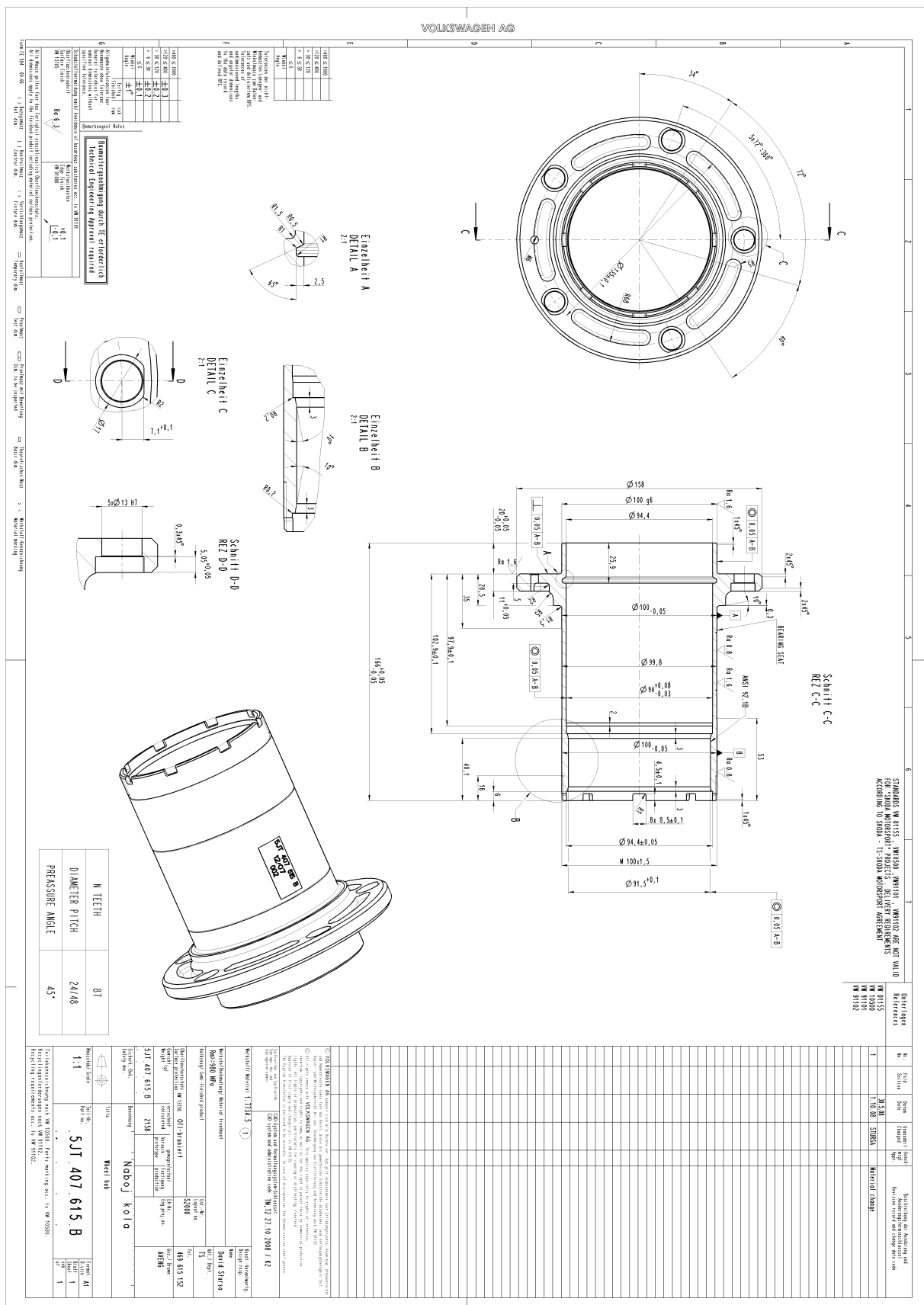


Figure A-5. Drawing Current Hub (Ljungberg, 2018)

Drawing Current Socket

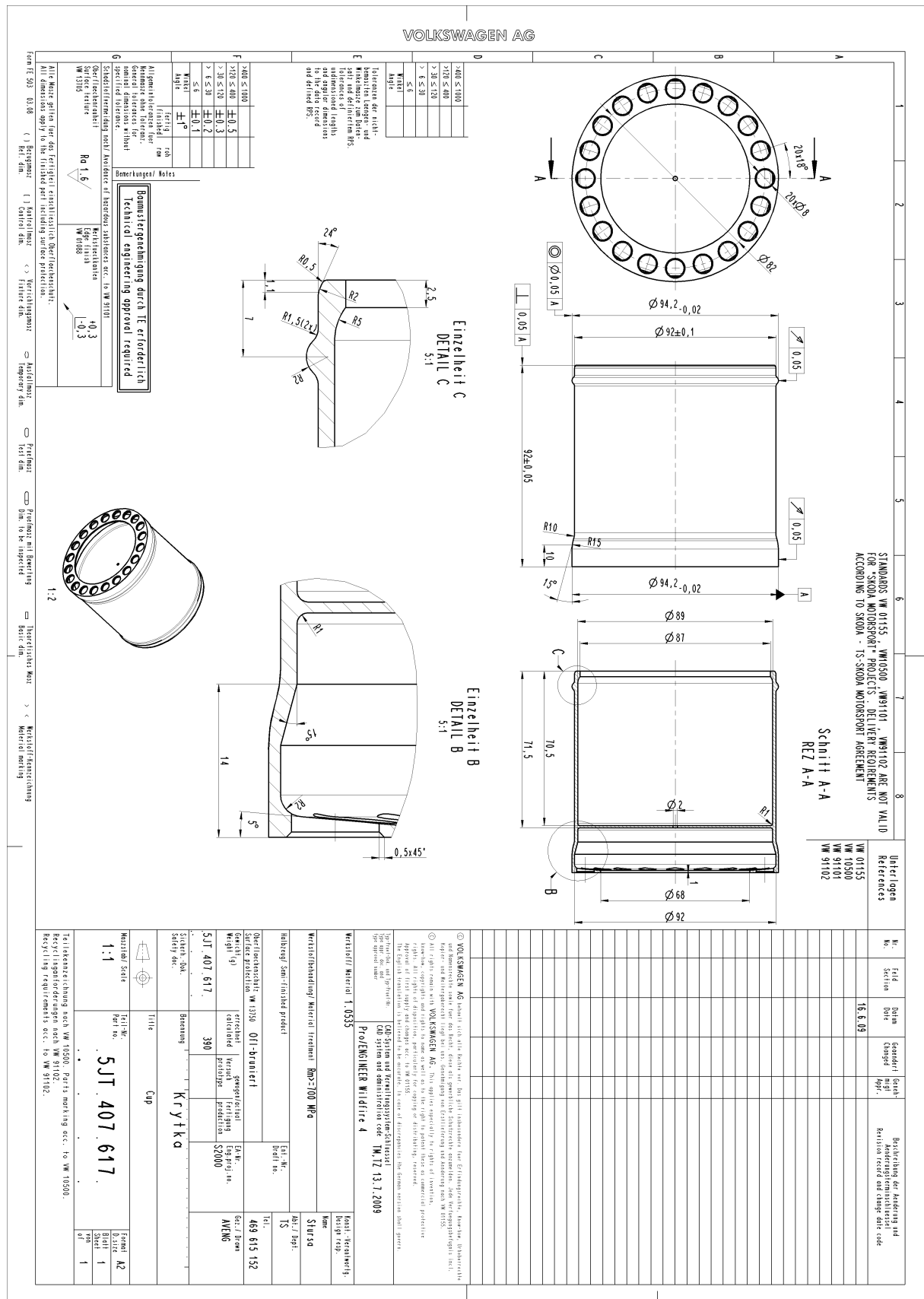


Figure A-6. Drawing Current Socket (Ljungberg, 2018)

Drawing Brake Disk from Brembo®

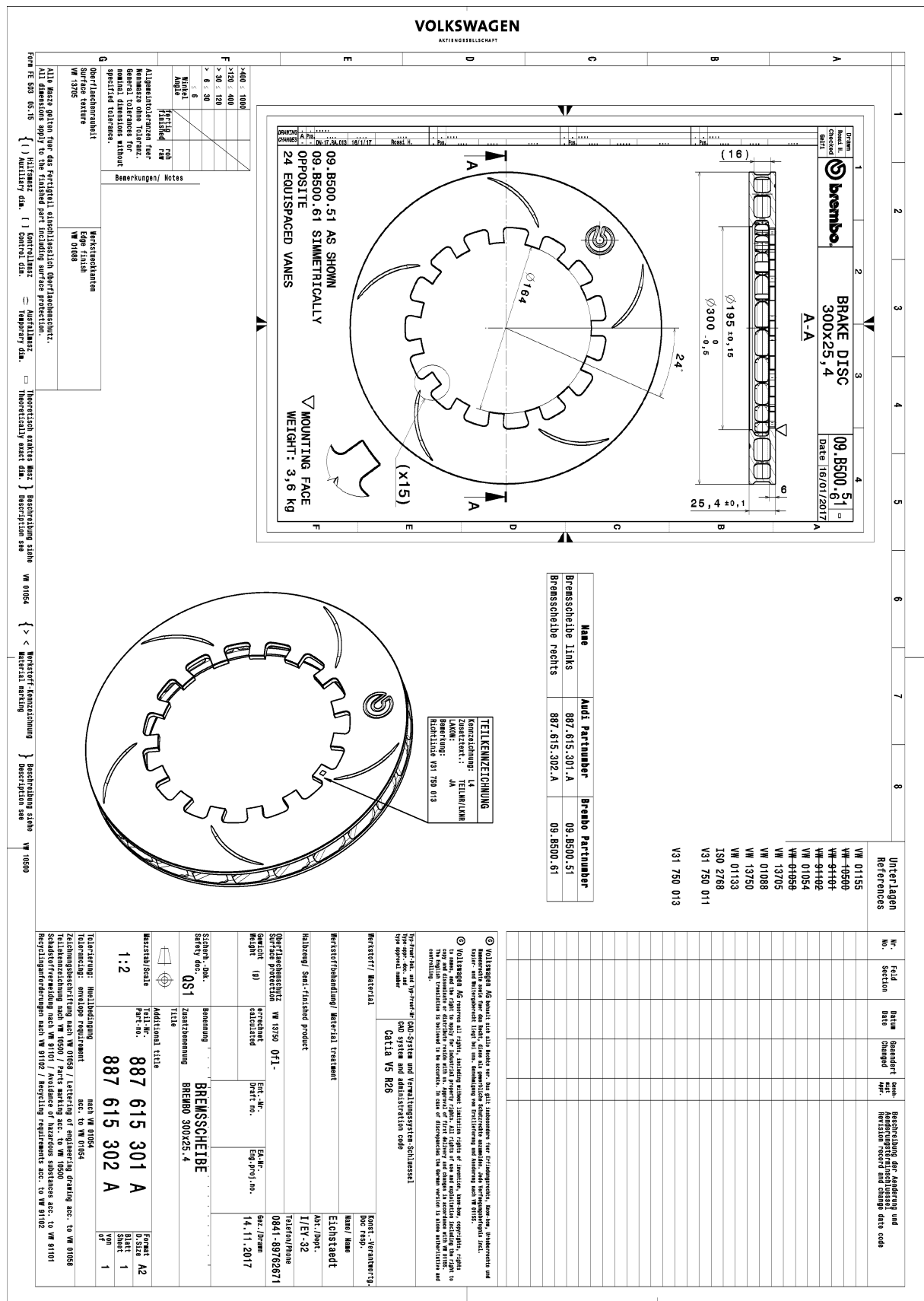


Figure A-7. Drawing Brake Disk from Brembo® (Ljungberg, 2018)

